



NACA TN 2675

590

NATIONAL ADVISORY COMMITTEE FOR AERONAUTICS

TECHNICAL NOTE 2675

MEASUREMENTS OF FLYING QUALITIES OF AN F-47D-30 AIRPLANE
TO DETERMINE LATERAL AND DIRECTIONAL STABILITY
AND CONTROL CHARACTERISTICS

By R. Fabian Goranson and Christopher C. Kraft, Jr.

Langley Aeronautical Laboratory
Langley Field, Va.



Washington

July 1952

AFMCC
TECHNICAL LIBRARY

AFL 2811



0065459

12

NATIONAL ADVISORY COMMITTEE FOR AERONAUTICS

TECHNICAL NOTE 2675

MEASUREMENTS OF FLYING QUALITIES OF AN F-47D-30 AIRPLANE
TO DETERMINE LATERAL AND DIRECTIONAL STABILITY
AND CONTROL CHARACTERISTICS¹

By R. Fabian Goranson and Christopher C. Kraft, Jr.

SUMMARY

Flight tests were made to determine the lateral and directional stability and control characteristics of an F-47D-30 airplane. The results of these tests showed the airplane stability to be weak directionally in low-speed conditions. In the power-off landing condition and high-speed clean conditions, the directional stability was satisfactory. The effect of increasing the altitude was to decrease the stability. The general characteristics of the aileron control were satisfactory, but the values of the aileron effectiveness were low and failed to meet the Air Force handling-qualities requirements. The rudder-force trim change with change in power and speed was rather large and objectionable to the pilot, although the forces encountered did not exceed the specified requirements.

INTRODUCTION

This paper presents an investigation of the flying qualities of the F-47D-30 airplane. Many flying-qualities investigations have been conducted by the National Advisory Committee for Aeronautics with various types of airplanes and this paper is intended to supplement this information. By correlation of these data with pilot opinions of these airplanes, it has been possible to establish quantitative requirements for satisfactory handling qualities such as those presented in reference 1. Additional information is continually being obtained, however, to determine whether the existing requirements are adequate or whether they should be modified in order to provide for conditions encountered

¹Supersedes the recently declassified NACA RM L6L31 for the Air Materiel Command, Army Air Forces, "Measurements of Flying Qualities of a P-47D-30 Airplane (AAF No. 43-3441) To Determine Lateral and Directional Stability and Control Characteristics" by R. Fabian Goranson and Christopher C. Kraft, Jr., 1947.

with airplanes of later design. Flight tests of the hinge-moment characteristics of the F-47D Frise type ailerons (measured individually) are also presented. These ailerons had been modified to correspond to a design recommended and tested by the NACA. A comparison between the data obtained from these tests and those obtained from previous NACA wind-tunnel tests of these ailerons is also presented. This paper presents the data for the lateral and directional stability and control characteristics of this airplane, as well as measurements of the aileron hinge-moment characteristics.

DESCRIPTION OF AIRPLANE AND TESTS

The F-47D-30 is a low-wing fighter-type airplane. This model incorporates an R-2800-59 engine, a dorsal fin, dive-recovery flaps, round-nose Frise ailerons, and a bubble canopy. A three-view drawing of the airplane is shown in figure 1 and additional data describing the airplane are presented in table I. Photographs of the test airplane are shown in figures 2 to 4. The airplane was flown at the forward center-of-gravity position of 26.4 percent mean aerodynamic chord with the landing gear down or 26.0 percent mean aerodynamic chord with the landing gear up with the gross weight varying from 12,310 pounds to 11,870 pounds. This forward center-of-gravity position of 26.4 percent mean aerodynamic chord was obtained by flying the airplane with the auxiliary tank empty and by attaching approximately 200 pounds of lead to the propeller-reduction-gear box. The lead installation is shown in the photographs of figure 5. This center-of-gravity position was used to obtain a larger degree of longitudinal stability since the airplane was known to be longitudinally unstable with power on in the center-of-gravity range obtainable with the normal loadings. The installation of instruments caused a rearward shift of the center of gravity of only 0.2 percent of the mean aerodynamic chord. The center-of-gravity position with the lead ballast and instruments installed was 0.8 percent of the mean aerodynamic chord in front of the most forward center-of-gravity position of the normally loaded airplane. The forward center-of-gravity position of 24.75 percent of the mean aerodynamic chord given by the airplane manual could not be obtained in the test airplane with any normal loading. The lateral center-of-gravity position was the same as that of the airplane in the service condition. The airplane was symmetrically loaded and wing fuel tanks were not used during the test program in order to eliminate any lateral center-of-gravity shift during flight.

Tests were run at low altitude in the conditions as shown in the following table:

Condition	Power	Flaps	Gear	Canopy
Approach	21 in. Hg at 2550 rpm	Down	Down	Open
Glide	Off	Up	Up	Closed
Landing	Off	Down	Down	Open
Power-on clean	42.5 in. Hg at 2550 rpm	Up	Up	Closed
Wave-off	42.5 in. Hg at 2550 rpm	Down	Down	Open

Tests were also run at high altitude in the power-on clean and glide conditions.

Most of the sideslip data presented were obtained by the steady-sideslip method where the pilot sideslipped the airplane to a certain angle and, when the airplane reached a steady condition, a record was taken of the required values. In some cases the method of continuous sideslip was used to obtain the data. In this method the airplane was sideslipped through a given range of sideslip angles at a rate not exceeding $\frac{1}{2}^{\circ}$ change in sideslip per second, and the various required values were recorded throughout the entire period. The data obtained by the continuous-sideslip method are indicated in this paper by flagged symbols.

INSTRUMENTATION

Standard NACA photographically recording instruments were used to obtain the data. The pilot's notes of indicated readings of the instruments in the cockpit of the fuel quantities, altitude, and free-air temperature were also used. The following recording instruments were installed in the test airplane:

- Accelerometer (three component)
- Stick-force recorder
- Rudder-pedal-force recorder
- Airspeed recorder
- Roll turnmeter
- Pitch turnmeter
- Yaw turnmeter
- Recording inclinometer (angle of bank)
- Sideslip-angle recorder
- Control position recorders
- Timer (synchronizing all records)

The yaw vane used to measure the angle of sideslip was mounted on a boom 1 chord ahead of the left wing tip. The term, indicated sideslip, used in this paper, is the uncorrected reading given by the yaw vane. The changes in sideslip angle obtained from the yaw vane are believed to be correct but the absolute magnitude of sideslip angle may be in error by a small amount because of lack of symmetry of the yaw vane or because of angularity of flow at the yaw vane. The airspeed was measured by means of a swiveling static head and a shielded total head mounted on a boom 1 chord ahead of the right wing tip. These instrument installations are shown in figure 2. The airspeed installation was calibrated for position error. The position error at low speeds was determined by flying the test airplane in formation with another airplane with an airspeed measuring system which had been calibrated with a trailing airspeed head. At high speeds the position error was determined by the fly-by method as described in reference 2. The term, calibrated airspeed, as used in this paper, may be defined by the following equation:

$$V_c = 45.08 f_o \sqrt{q_c}$$

where

- V_c calibrated airspeed in miles per hour; that is, the reading in miles per hour that would be given by a standard Army-Navy airspeed meter if it were connected to a pitot-static system free from position error
- f_o standard sea-level compressibility correction factor
- q_c pressure differential, in inches of water, between total and static head, corrected for position error

The apparatus used to calibrate the strain gages in the ailerons that measured the aileron hinge moments is shown in figure 6.

RESULTS AND DISCUSSION

Physical Characteristics

The physical characteristics of the rudder, aileron, and elevator control systems as measured on the ground are shown in figures 7 to 12. The variation of the elevator and aileron deflections with stick angle is shown in figure 7 and the friction in these two control systems

is shown in figure 8. The friction in both the elevator and aileron control systems was small and well within the requirements of reference 3. The characteristics of the rudder control system are shown in figures 9 to 12. The variation of the rudder position with pedal position is shown in figure 9 and the variation of the rudder tab angle with rudder angle for the three tab-angle settings is shown in figure 10. The friction in the rudder control system (fig. 11) is approximately ± 10 pounds. The restoring force of approximately 20 pounds at full deflection of the rudder control system was created by springiness of the control system. The stretch in the rudder control system is shown in figure 12 and indicates a loss of 5° of rudder deflection per 100 pounds of rudder force.

Static Directional and Lateral Stability and Control Characteristics

Static directional stability and control data are presented in figures 13 to 19 and the adverse aileron yaw and rudder power are shown in figures 20 and 21.

The static-directional-stability data show the variation of rudder angle with sideslip angle at small angles of sideslip to be approximately 0.58 in the low-speed (150 mph) power-on clean condition (fig. 15(a)) and 0.30 in the low-speed (150 mph) glide condition (fig. 13(a)). In the low-speed (150 mph) glide condition the airplane exhibits zero change in rudder force for small angles of left sideslip. These undersirable characteristics are not encountered, however, at the higher speeds tested (fig. 13(b)). A similar condition exists at high altitude (figs. 14(a) and 14(b)).

In the low-speed, low-altitude, power-on clean condition (fig. 15(a)), the airplane exhibits zero stick-free dihedral effect beyond 10° sideslip to the left and right and zero or negative rudder-force gradient between 5° and 10° left sideslip. These objectionable characteristics disappear at the higher speeds (figs. 15(b) and 15(c)). The effect of altitude in the power-on clean condition (fig. 16(a)) is to decrease the directional stability with the parameter $\partial\delta_r/\partial\beta$ (where δ_r is the rudder angle and β is the sideslip angle) decreasing from 0.58 at low altitude to 0.45 at high altitude at 150 miles per hour. Zero rudder force is required to reach 22° left sideslip and zero stick-free dihedral effect is indicated beyond 5° left and right sideslip. A comparison of the sideslip data obtained from wind-tunnel tests and the flight tests shown in this paper is made in figure 19 by the method given in reference 4. The wind-tunnel data in the power-on clean condition obtained from reference 5 correspond to a flight speed of approximately 326 miles per hour and these data are compared with the 270-mile-per-hour and 350-mile-per-hour power-on clean flight test data. This

comparison shows the data to be in fair agreement since the parameter $\partial\delta_r/\partial\beta$ for the wind-tunnel tests is 0.875 and is approximately 0.70 for the 270-mile-per-hour and 350-mile-per-hour flight test data. This difference can be accounted for by the difference of the two configurations that were tested. The wind-tunnel model was similar to an F-47B; whereas the F-47D-30 tested in flight had a bubble canopy, an increase in power, and a propeller of different design.

The directional characteristics in the power-off landing condition (fig. 17) are satisfactory. In the 120-mile-per-hour wave-off condition (fig. 18(b)), the stick-free dihedral effect is negative beyond 5° right sideslip and becomes negative everywhere at the lower speed of 100 miles per hour (fig. 18(a)). This negative stick-fixed dihedral effect in the wave-off condition was also predicted by the wind-tunnel tests of reference 5. The wind-tunnel tests indicated approximately 5° of negative dihedral in this condition which is approximately the same as that obtained in flight. (See fig. 18(a).) A comparison of wind-tunnel test data and flight data in sideslips is made in figures 19(b) and 19(c) for the landing and wave-off conditions. The slopes of the curves of the rudder-angle variation with sideslip angle are in very good agreement, the wind-tunnel and flight-test parameter $\partial\delta_r/\partial\beta$ for the landing condition being 1.0 and 0.92, respectively, and for the wave-off condition 1.2 and 1.23, respectively. This slight difference can also be accounted for by the reasons in the preceding paragraph.

In order to determine the change in sideslip angle during abrupt aileron rolls, the airplane was rolled out of 45° banked turns with the ailerons deflected various amounts and the rudder held fixed. The rolls were made in both the landing and power-on clean conditions. These data (fig. 20) indicate that slightly more than 1° of sideslip results with 5 percent of full aileron deflection in the clean condition. In order to determine the power of the rudder to overcome adverse aileron yaw, the airplane was rolled by simultaneously applying full aileron deflection and various amounts of rudder to full rudder deflection. Zero yaw could not be maintained in this maneuver because of physical restrictions in the cockpit. The large stick movement necessary to obtain full aileron deflection interfered with the pilot's leg movement, so that in left rolls it was necessary to limit the aileron travel to approximately $4/5$ of full deflection in order to apply rudder and aileron deflection simultaneously. From these data, figure 21, it is questionable whether the rudder is powerful enough to overcome the adverse yaw due to full aileron deflection since the pilot applied approximately 150 pounds of pedal force in trying to maintain zero yaw which resulted in a loss of approximately 7° of rudder deflection due to the stretch in the control system. (See fig. 12.)

Dynamic Directional Stability and Control Characteristics

Dynamic directional stability characteristics are shown in the time histories of typical directional oscillations in figures 22 to 25. In the power-on conditions, large pitching moment due to sideslip inherent in this airplane and small or negative dihedral effect caused the airplane to diverge longitudinally or spirally at low speeds whether the oscillation was started from a small angle of sideslip or by a rudder kick. This divergence was often rapid and hard to control. No oscillation of the rudder occurred for any of the conditions tested.

Directional and Lateral Trim Characteristics

Trim changes due to power changes were measured at airspeeds simulating approach, best climb, maximum level flight with rated power, and maximum range with power for maximum range. The measured force changes for these conditions are shown in table II and indicate that the permissible rudder force of 180 pounds was not exceeded; however, the amount of force was objectionable to the pilot. The rudder-force variation with speed is shown in figure 26. The forces at high speeds were high but did not exceed the 180-pound limit set forth in the Air Force requirements. The rudder trim tab was capable of trimming the rudder forces to zero at all speeds except those below 120 miles per hour in the power-on clean condition. In both take-off and landing the rudder was adequate to control the airplane.

Aileron Control Characteristics

The aileron control power, stick forces, and hinge moments were measured in the landing and power-on clean condition. The variation of rolling acceleration with aileron deflection was always in the correct direction and the rolling velocity varied smoothly with aileron deflection. These characteristics can be seen in the time histories of figure 27. The variation of helix angle $pb/2V$ and aileron stick force with aileron deflection at various speeds are presented in figures 28 to 30, and a plot of the maximum values of $pb/2V$ obtainable with a 30-pound stick force as a function of speed is shown in figure 31. The data show the maximum $pb/2V$ to be 0.074 which is considerably lower than the Air Force requirement of a $pb/2V$ of 0.09. The variation of the $pb/2V$ obtainable with a stick force of 30 pounds with speed was also below the Air Force requirement (fig. 31).

The variation of aileron hinge-moment coefficients with aileron deflection is presented in figures 32 and 33. These data show a moment tending to cause the ailerons to float up at all the speeds tested.

Although the value of hinge-moment coefficient at zero aileron deflection decreased with increasing speed, the aileron hinge moment tending to cause the ailerons to float up was increasing. The hinge-moment coefficients become less negative at high Mach numbers but there is no effect on the slopes of the curves. It should be pointed out that the F-47D-30 ailerons are highly balanced and, if the control system were flexible, the ailerons would more than likely become overbalanced at high speeds. This tendency, which has been encountered with Frise type ailerons on other airplanes, is caused by the up-going aileron moving to larger deflections for a given deflection of the down-going aileron than would occur with a rigid control system. As a result the hinge moment of the down-going aileron, tending to return the system to neutral, is not sufficient to offset the hinge moment of the up-going aileron which gives an overbalancing moment. The hinge-moment data also show that the up deflection of the ailerons at which separation of flow would occur is not reached since the curves do not show an abrupt change in hinge moment.

The aileron trim tab was sufficiently powerful to trim the aileron forces to zero in all the configurations tested.

Wind-tunnel tests were made of an aileron similar to those used on the F-47D-30 airplane and a comparison of the two sets of data is made. The wind-tunnel data were obtained from reference 6. Profile drawings of the ailerons tested in the wind tunnel and in flight are shown in figure 34. This figure shows that the aileron contours were almost the same, but the hinge locations were slightly different. A comparison of the wind-tunnel and flight test data of the aileron hinge-moment characteristics is shown in figure 35. The flight data indicated a tendency of the ailerons to float up which was not shown by the wind-tunnel data. Near the maximum up deflection tested, the wind-tunnel data show a rapid increase in hinge moment, which indicates stalling of the aileron balance. This tendency was not encountered in flight even though the deflection range tested was approximately the same.

CONCLUSIONS

1. The airplane had weak directional stability characteristics, both rudder free and rudder fixed, in all low-speed conditions except in the power-off landing condition where stability was satisfactory. The directional stability at the higher speeds was satisfactory.

2. The effect of higher altitude, approximately 25,000 feet, was to decrease slightly the directional stability.

3. Neutral to negative stick-free dihedral effect was indicated in all low-speed conditions except in the power-off landing condition. This characteristic was most marked in the low-speed (100 mph) wave-off condition.

4. The rudder did not oscillate during the directional oscillations, started either from a rudder kick or a sideslip. In the low-speed power-on clean condition, the airplane diverged longitudinally or spirally. This divergence was often rapid and hard to control.

5. The rudder-force trim change, with change in power and with change in speed, was high and objectionable to the pilot. The rudder control for landing and take-off was adequate but, because of stretch in the control system, the rudder could not be deflected enough to overcome the adverse aileron yaw at 150 miles per hour in the power-on clean condition.

6. The aileron trim tab was sufficiently powerful to trim the airplane in all the configurations tested. The rudder trim tab was not effective below approximately 120 miles per hour in the power-on clean condition, but this condition was not objectionable to the pilot.

7. The general characteristics of the aileron control were good but the effectiveness of the ailerons was below the Air Force requirements. The maximum $p\delta/2V$ obtainable was 0.074 as compared with the Air Force requirement of 0.09.

Langley Aeronautical Laboratory
National Advisory Committee for Aeronautics
Langley Field, Va., February 13, 1947

REFERENCES

1. Gilruth, R. R.: Requirements for Satisfactory Flying Qualities of Airplanes. NACA Rep. 755, 1943. (Formerly NACA ACR, April 1941.)
2. Thompson, F. L., and Zalovcik, John A.: Airspeed Measurements in Flight at High Speeds. NACA ARR, Oct. 1942.
3. Anon.: Specification for Stability and Control Characteristics of Airplanes. SR-119A, Bur. Aero., April 7, 1945.
4. Kayten, Gerald G.: Analysis of Wind-Tunnel Stability and Control Tests in Terms of Flying Qualities of Full-Scale Airplanes. NACA Rep. 825, 1945. (Formerly NACA ARR 3J22.)
5. Recant, I. G.: Wind-Tunnel Tests of 1/6-Scale Model of Republic XP-47B Airplane with Power. NACA MR, Feb. 11, 1941.
6. Luoma, Arvo A.: Effect of Compressibility on Section Characteristics of an Airfoil with a Round-Nose Slotted Frise Aileron. NACA TN 1075, 1946.

TABLE I
 PERTINENT DIMENSIONS OF THE F-47D-30 AIRPLANE

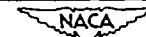
Engine	Pratt & Whitney R-2800-59
Propeller	(four blades) Curtiss Drawing No. SPA-5
Total wing area, sq ft	300
Total aileron area, sq ft	25.7
Aileron trim tab area (left aileron), sq ft	0.89
Stabilizer area, sq ft	33.0
Elevator area, sq ft	22.0
Elevator trim tab area, sq ft	0.94
Fin area, sq ft	13.9
Rudder area, sq ft	11.9
Rudder trim tab area, sq ft	0.87



TABLE II
 MEASURED FORCE CHANGES

Trim speed (mph)	Power change	Trim change due to power		
		Change in rudder force (lb)	Change in aileron force (lb)	Change in elevator force (lb)
128 (Approach)	Cut power Apply normal rated power	31 left 74 right	0 0.5 right	8.5 pull 20.5 push
158 (Best climb)	Cut power Apply normal rated power	31 left 72 right	1 right 0.5 left	6.1 pull 13.2 push
282 270 (Maximum level flight with normal rated power)	Cut power Apply normal rated power	21 left 70 right	0 0	1.5 pull 0
219 (Maximum range)	^a Cut power for maximum range ^a Apply power for maximum range	10.5 left 64 right	0.5 left 0	2.5 pull 3.9 push

^aPower for maximum range: 30 in. Hg manifold pressure, 1900 rpm, automatic lean.



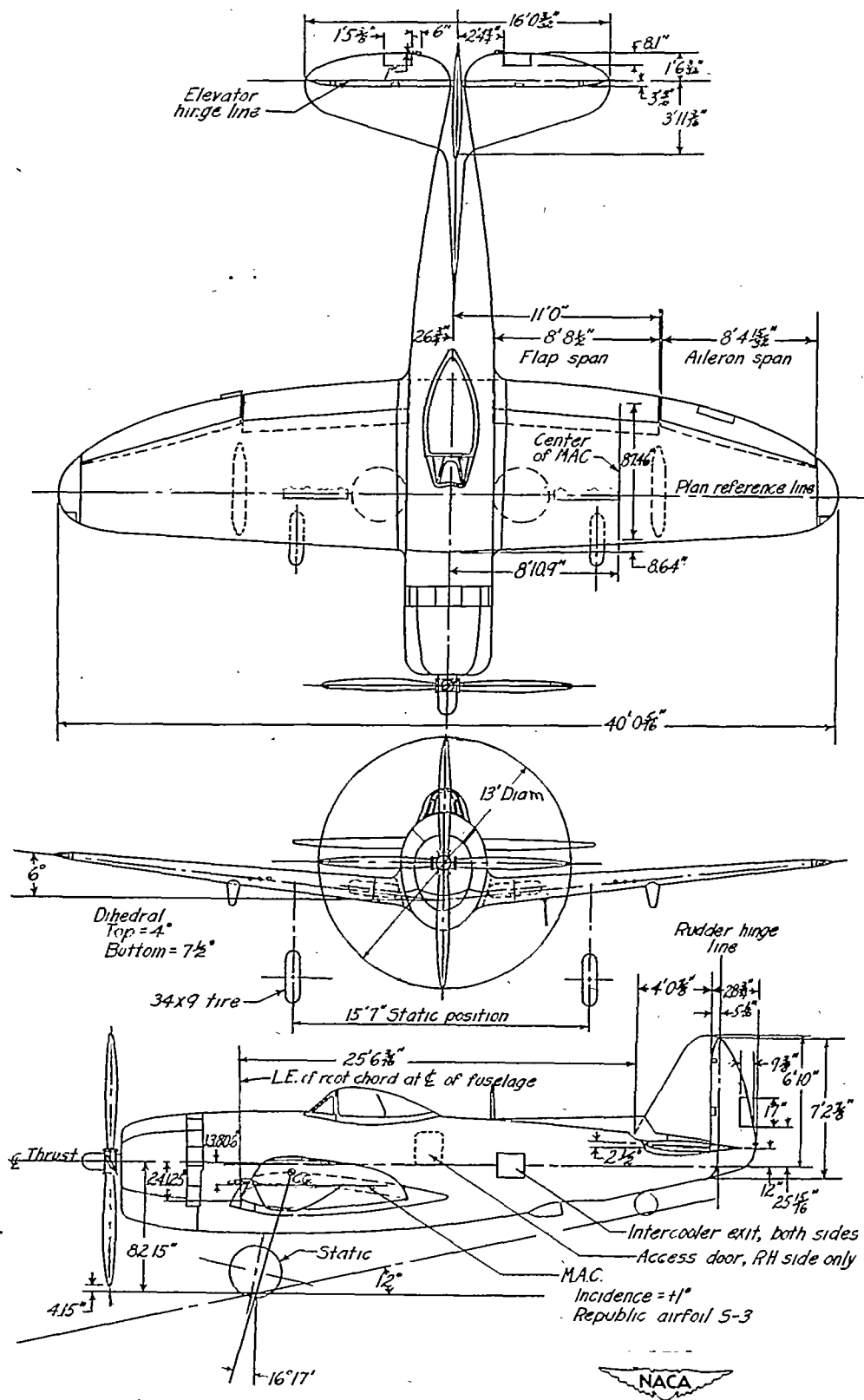


Figure 1.- Three-view drawing of the F-47D-30 airplane.

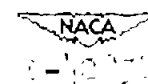


Figure 2.- Three-quarter front view of F-47D-30 test airplane.

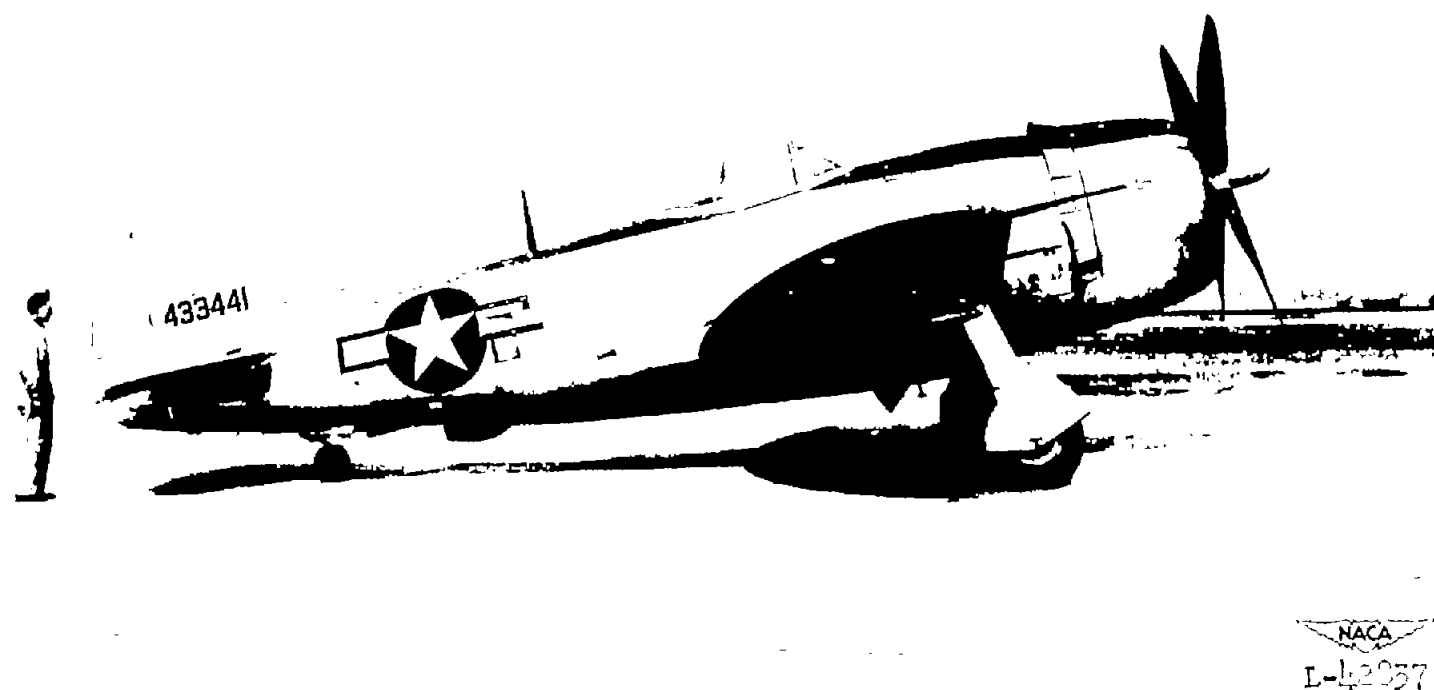
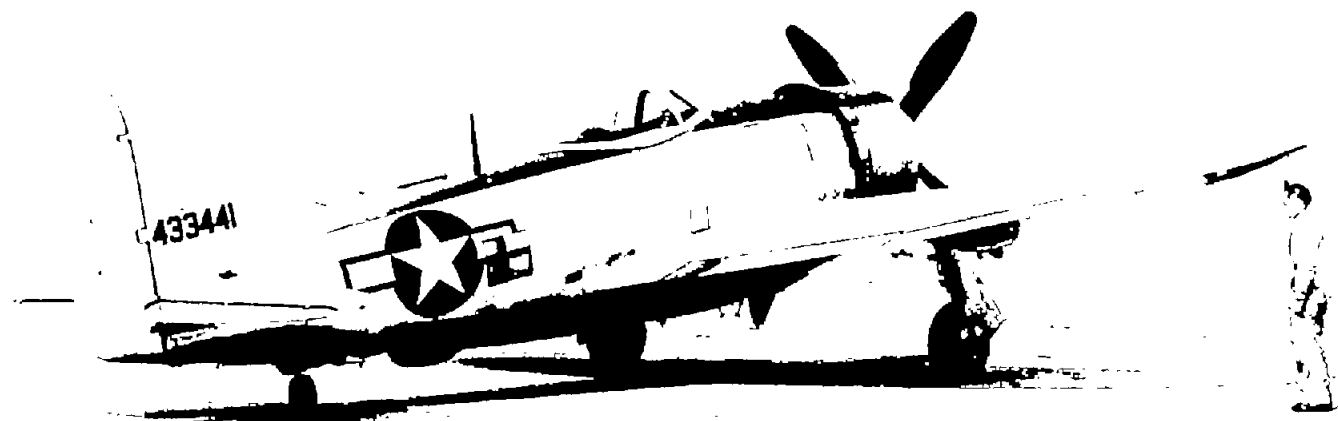


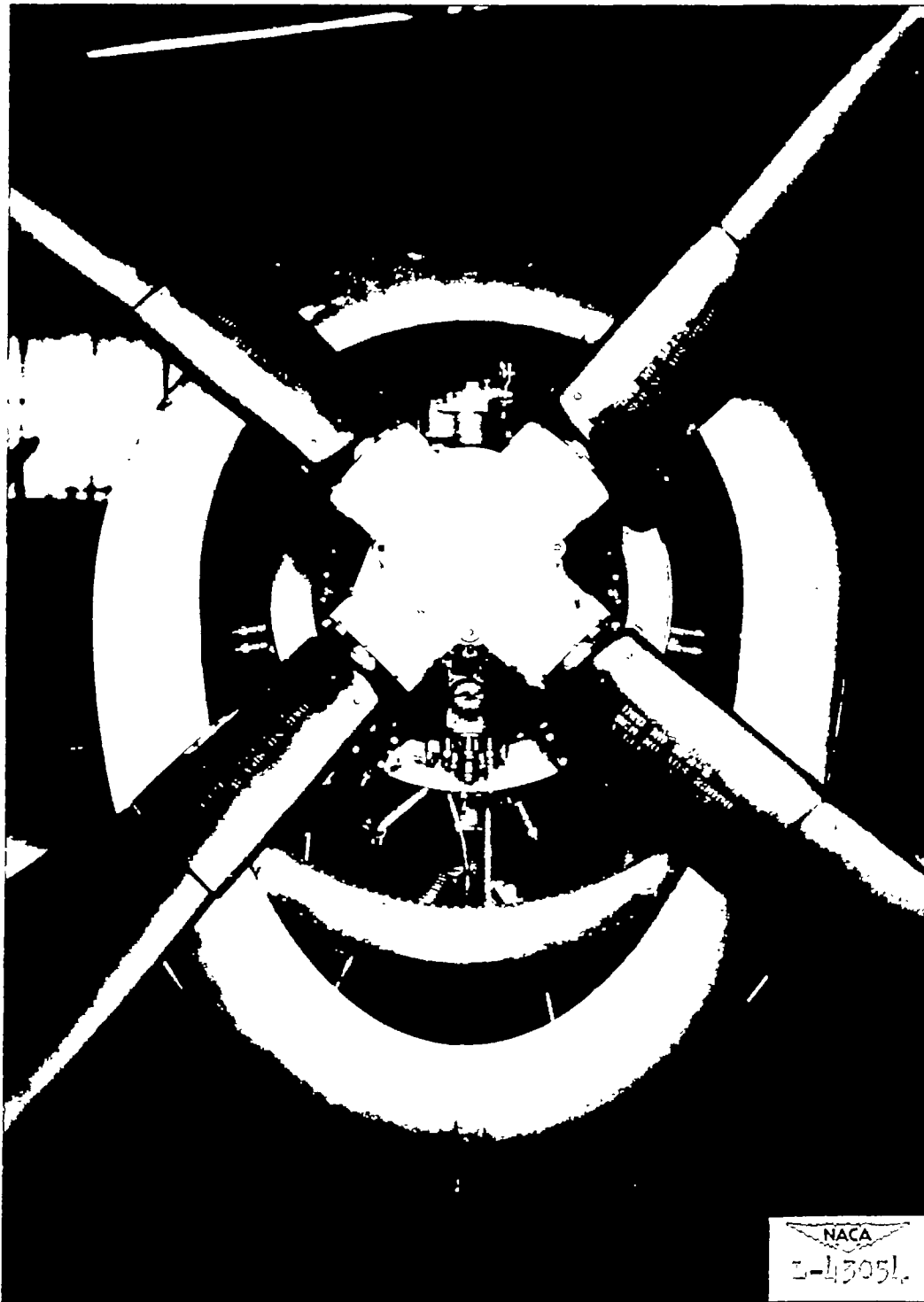
Figure 3.- Side view of F-47D-30 test airplane.

NACA TN 2675



NACA
2675

Figure 4.- Three-quarter rear view of F-47D-30 test airplane.

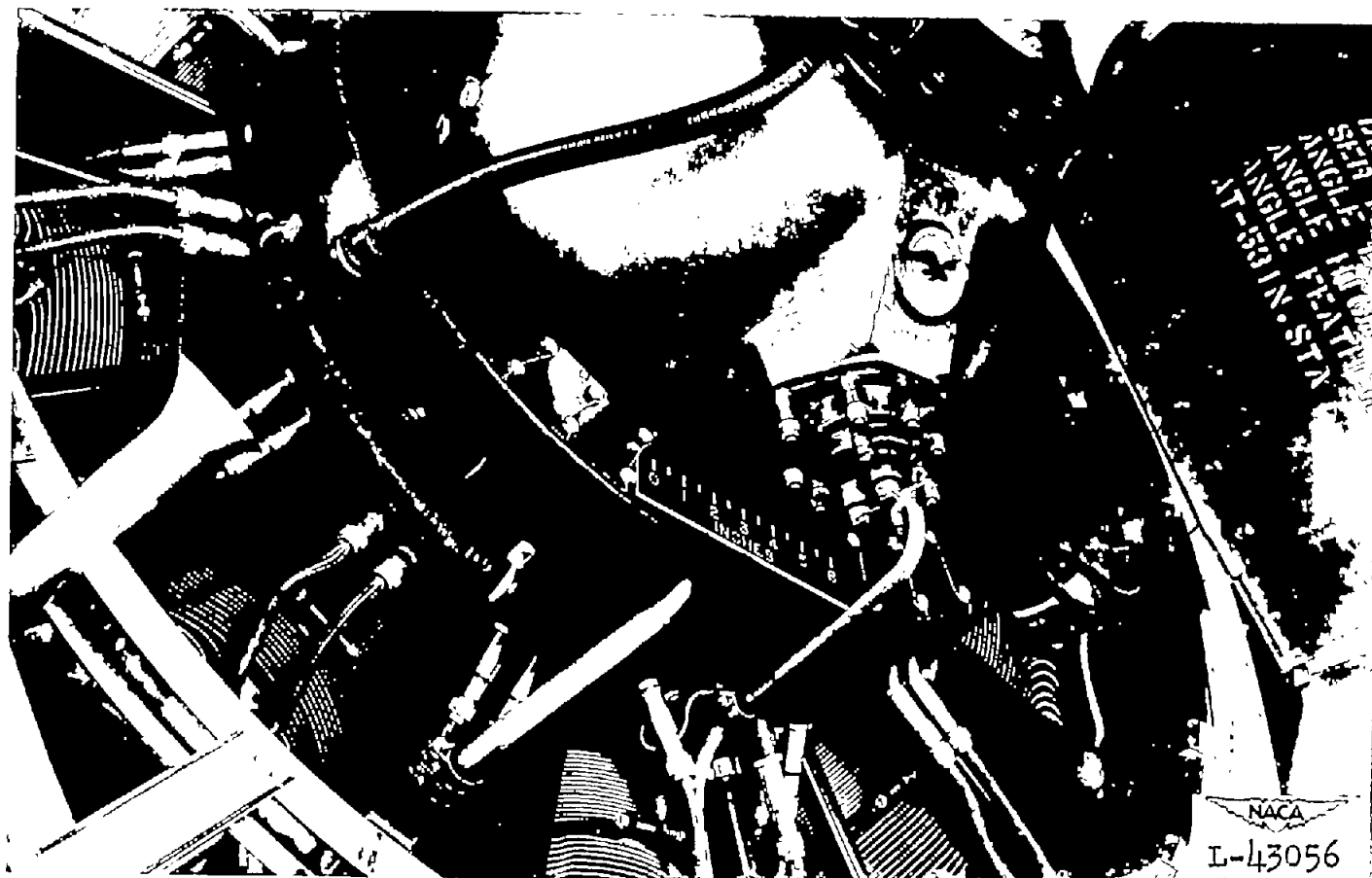


(a) Front view of engine showing lead ballast ring mounted on gear box.

Figure 5.- Photographs of ballast installed on F-47D-30 test airplane.

3Z

NACA TN 2675



(b) Details of lead ring mounted on reduction-gear housing.

Figure 5.- Concluded.

17

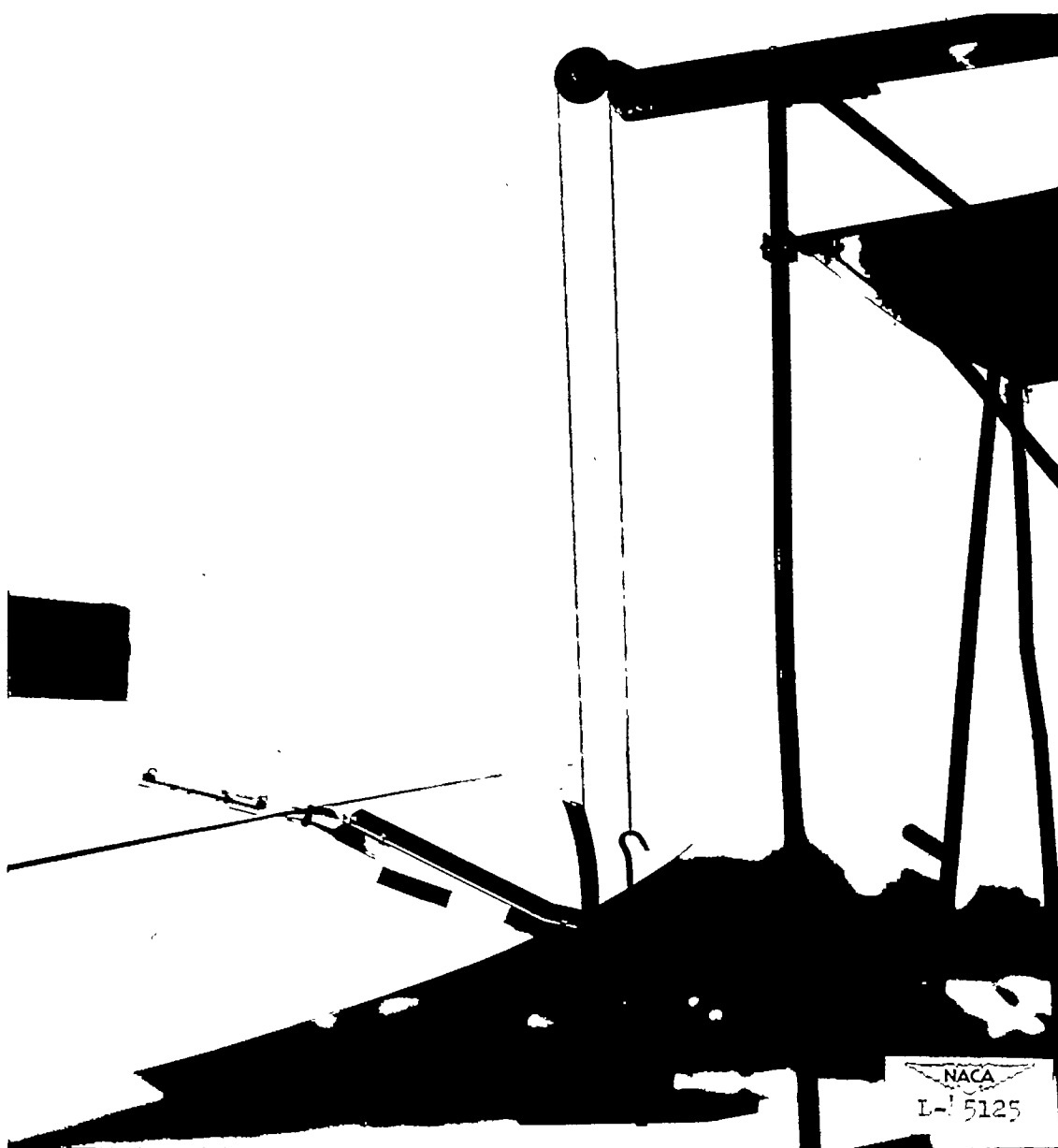


Figure 6.- Setup for calibrating aileron hinge-moment recorders.

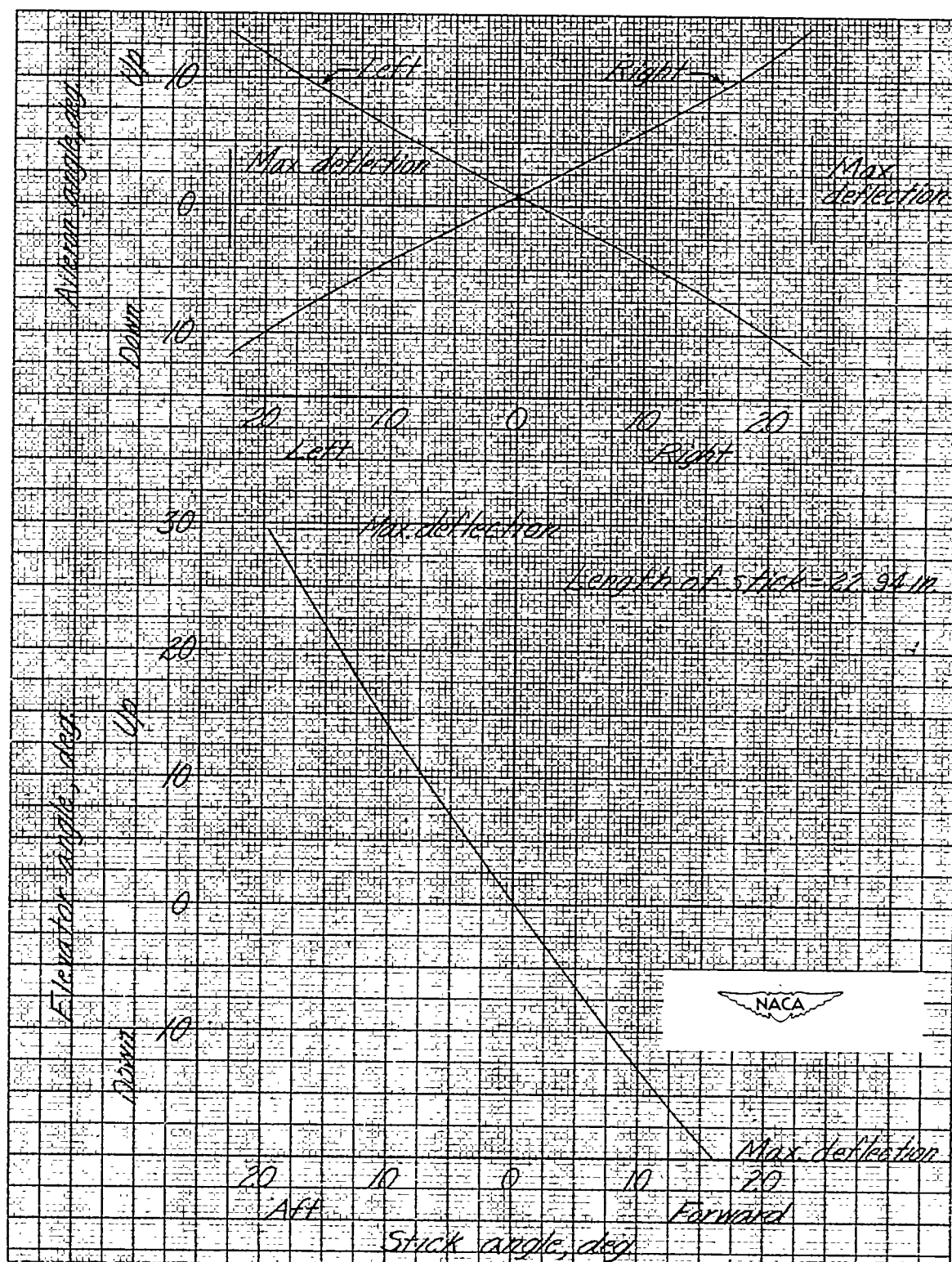


Figure 7.- Variation of aileron and elevator deflection with stick position. F-47D-30 airplane.

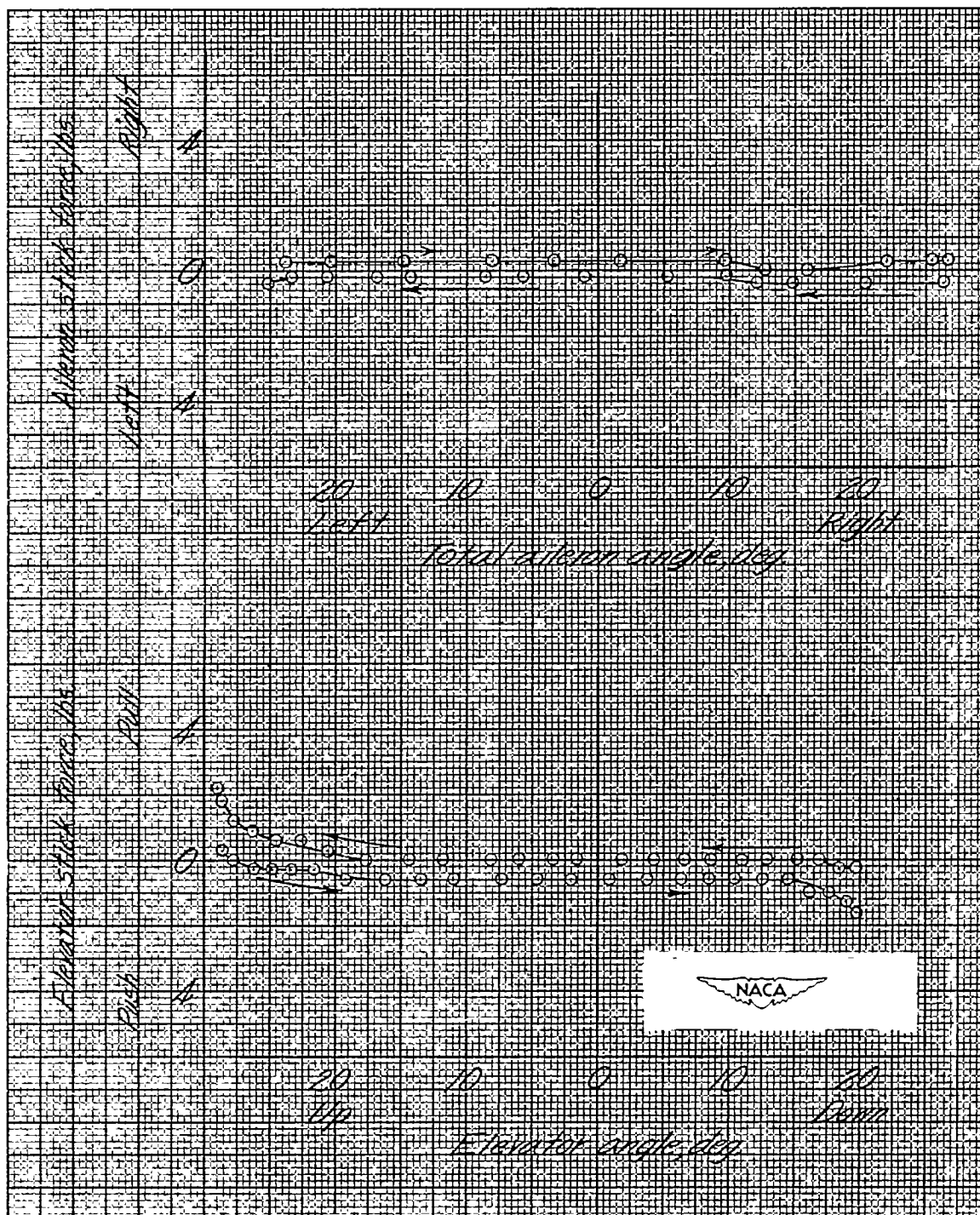


Figure 8.- Aileron and elevator stick force due to friction as measured on the ground in the three-point attitude with no load on the ailerons or elevator. F-47D-30 airplane.

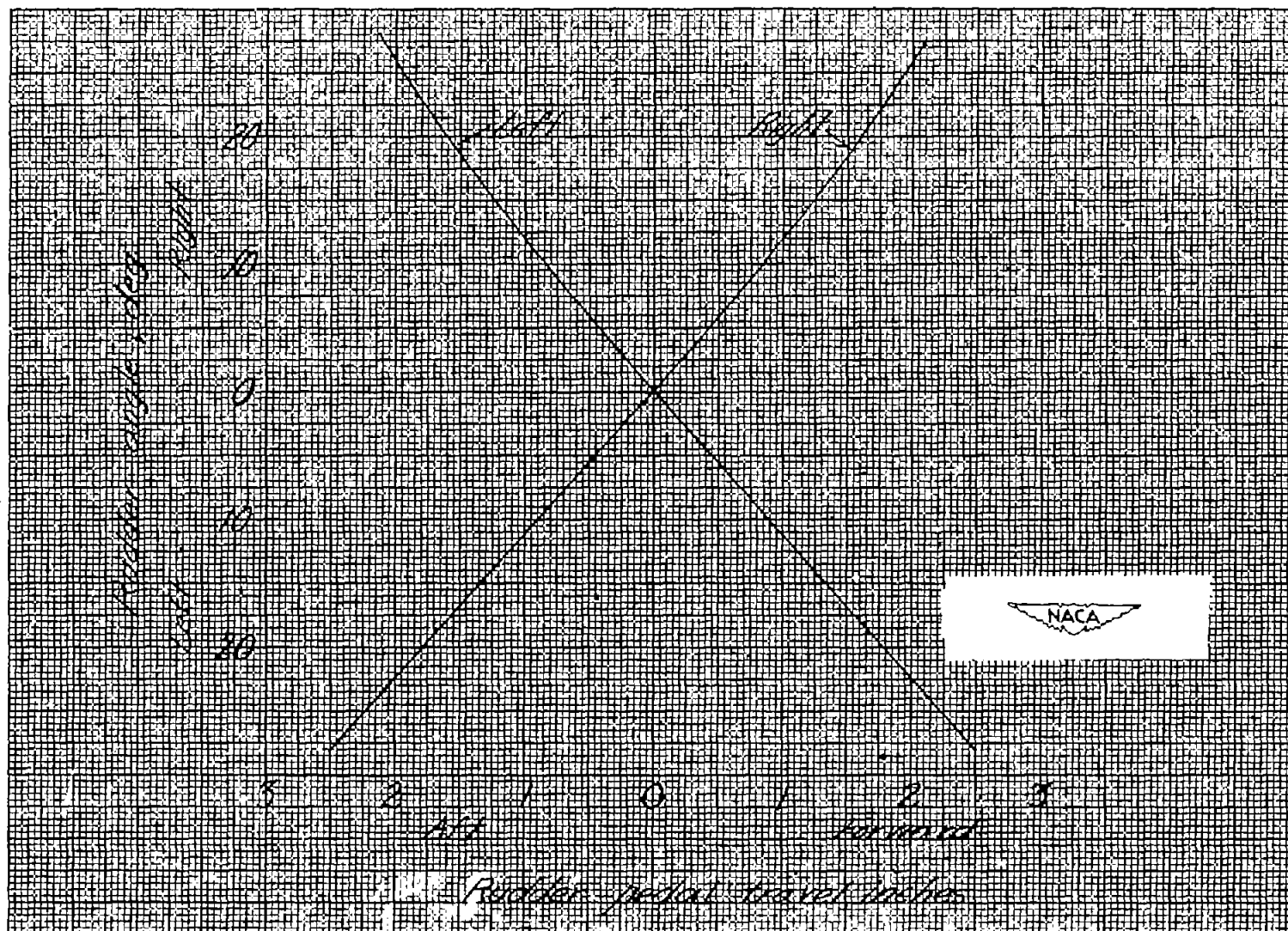


Figure 9.- Variation of rudder angle with rudder-pedal position as measured on the ground with no rudder load.

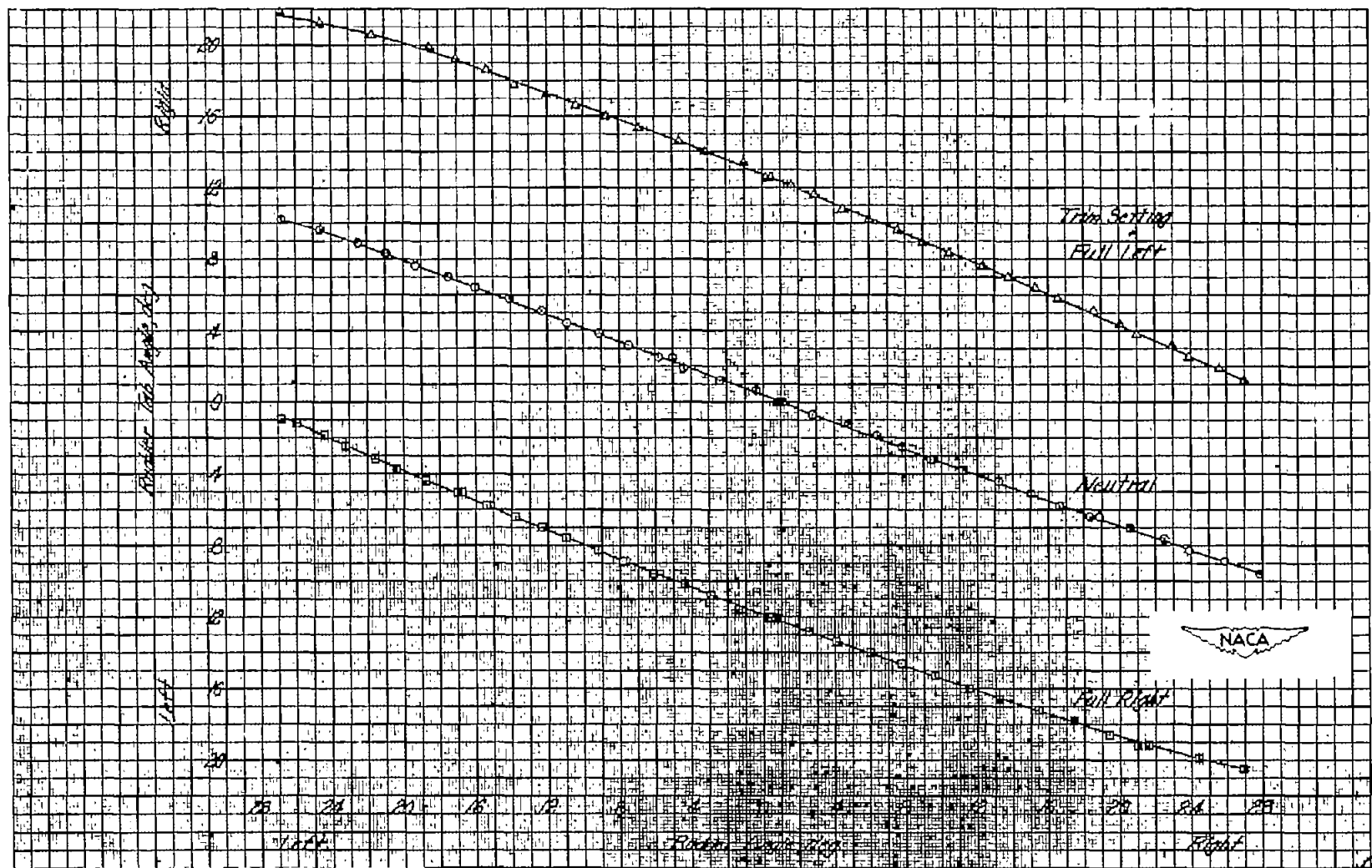


Figure 10.- Variation of rudder balancing tab angle with rudder angle for various trim settings. (Rudder tab is a combination trim and balancing tab.)

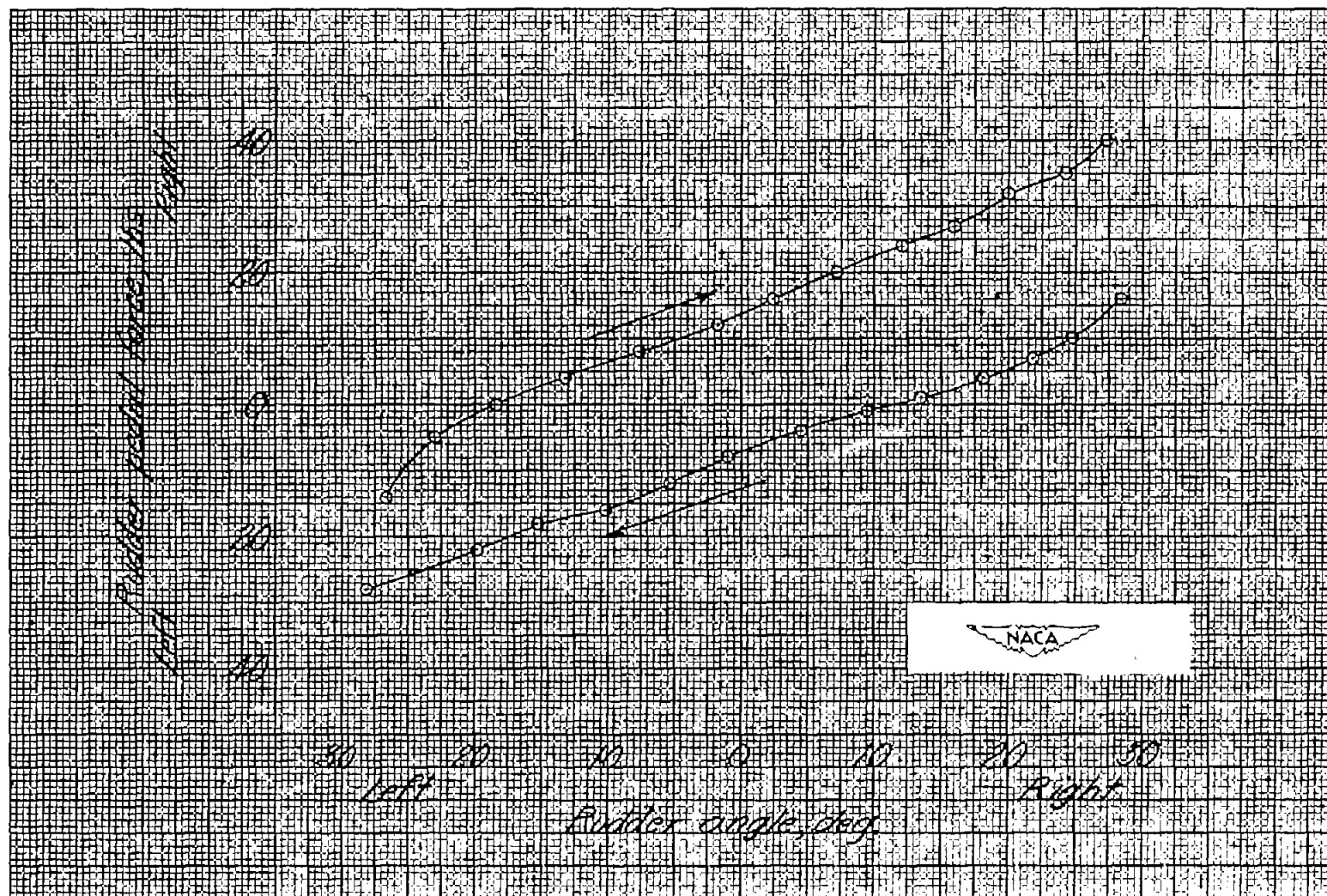


Figure 11.- Rudder-pedal forces due to friction in the rudder control system as measured on the ground with no rudder load. Free-air temperature 70° F.

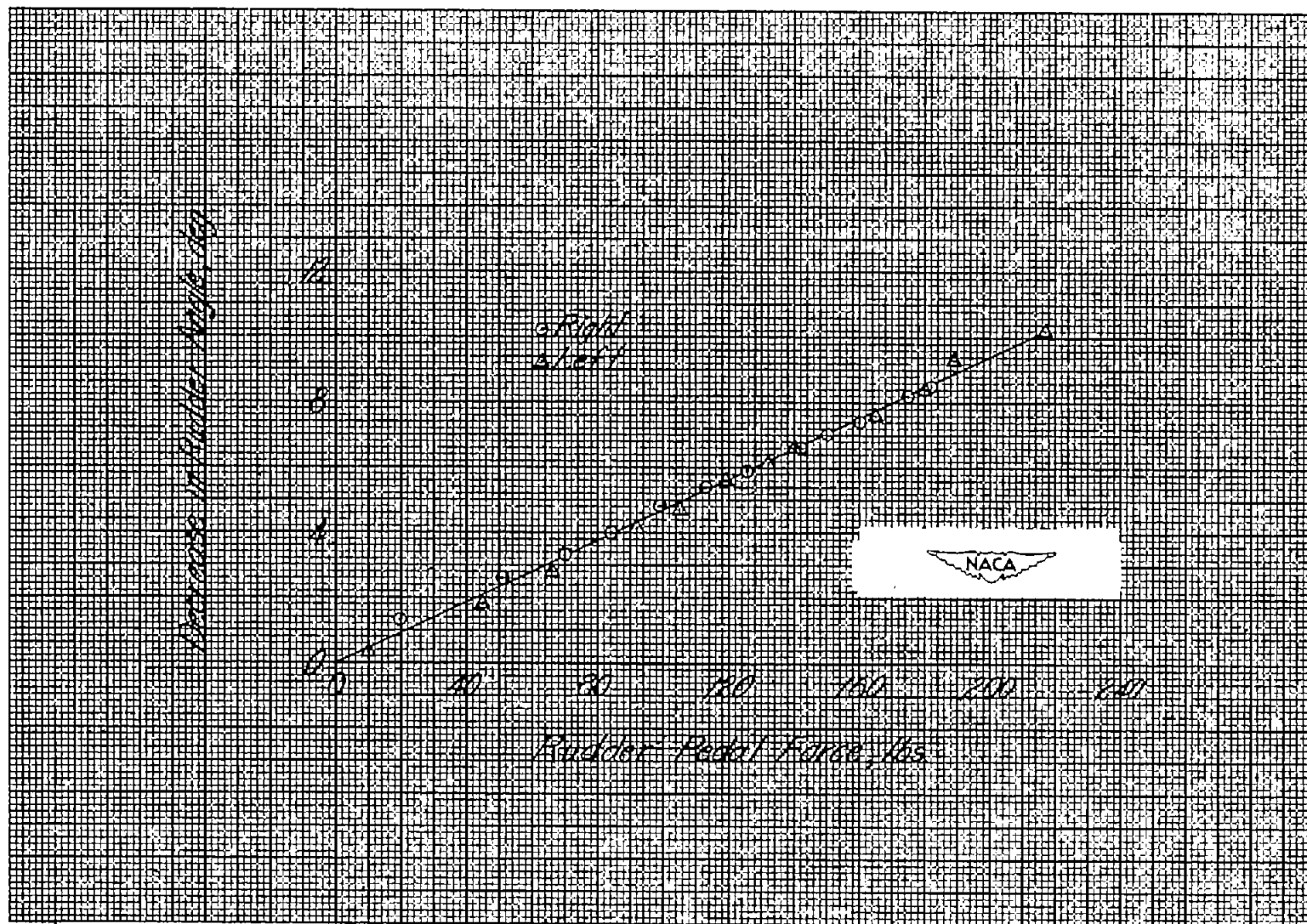
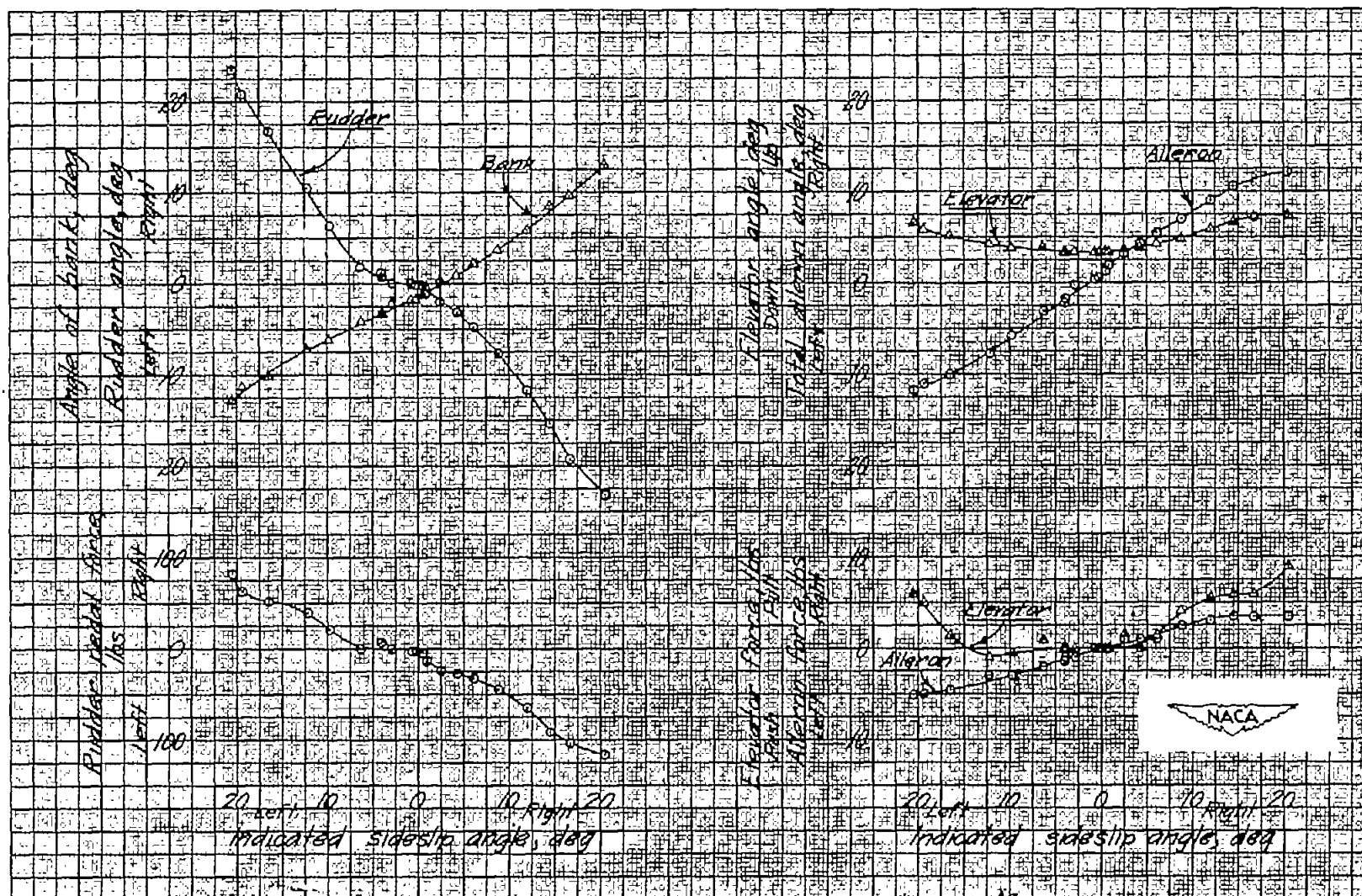
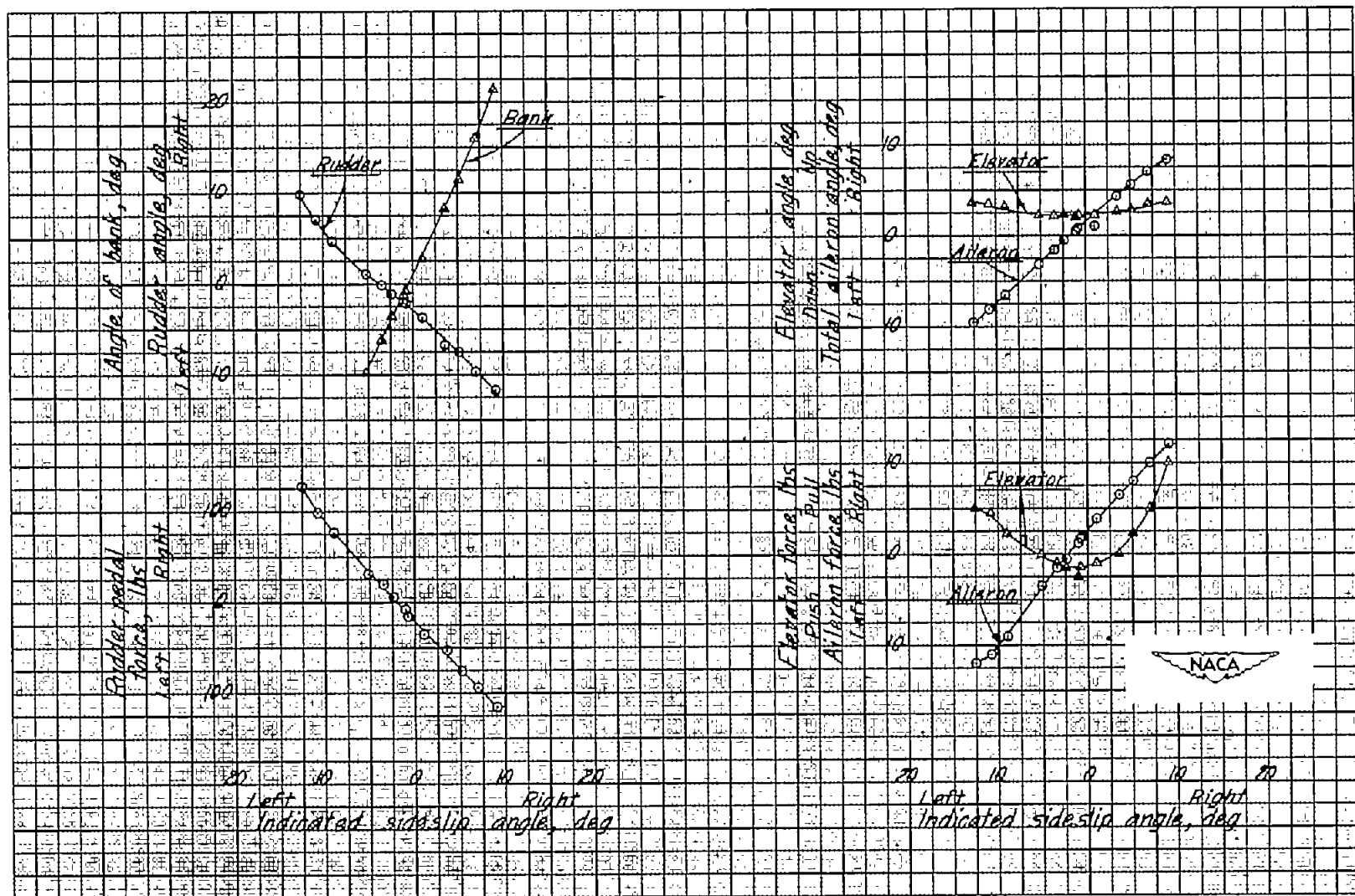


Figure 12.- Decrease in rudder angle due to stretch in the control cables.



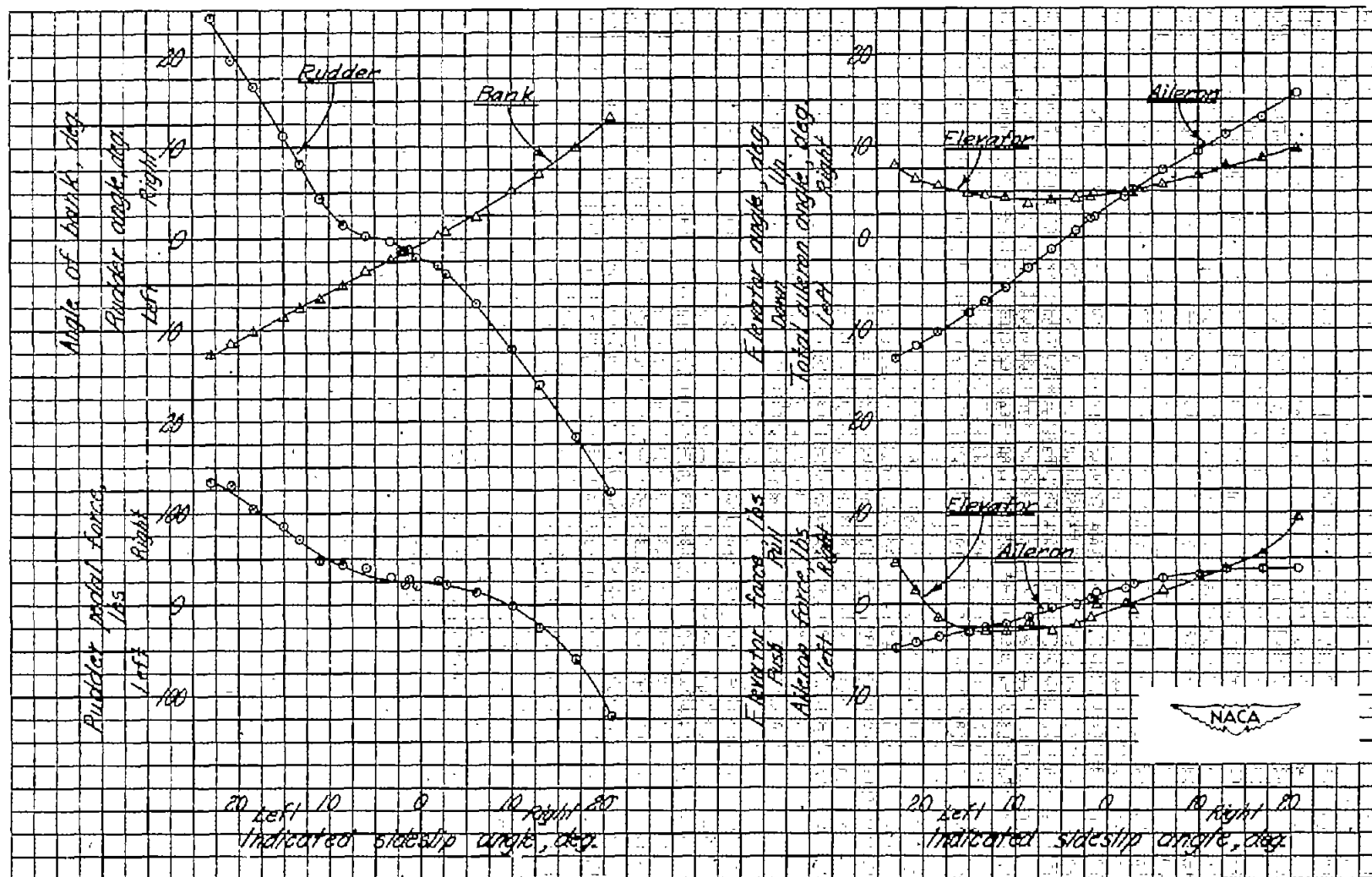
(a) 146-mile-per-hour calibrated airspeed at 6000 feet average altitude.

Figure 13.- Directional stability and control characteristics of the F-47D-30 in the glide condition at low altitude.



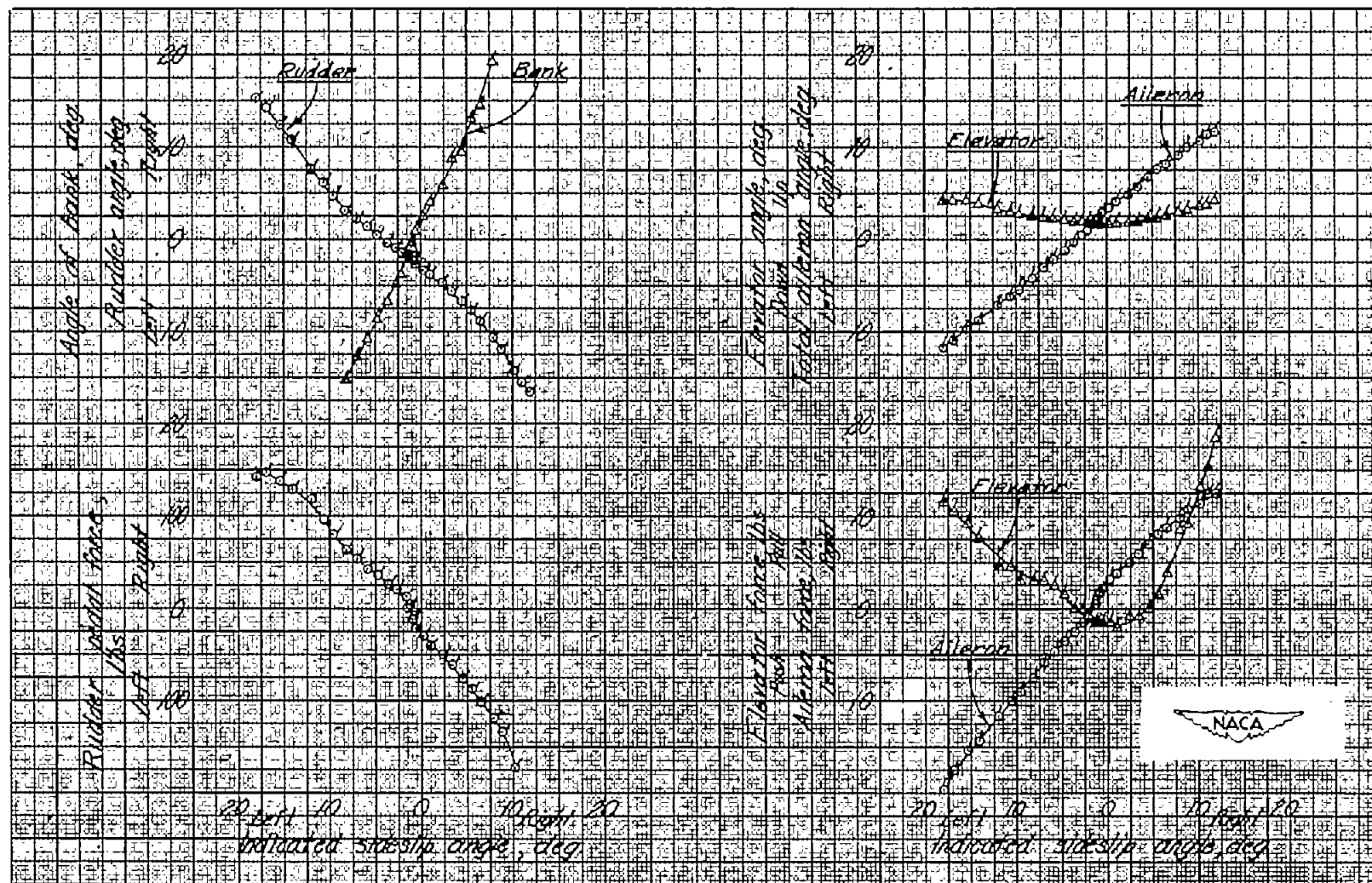
(b) 270-mile-per-hour calibrated airspeed at 5000 feet altitude.

Figure 13.- Concluded.



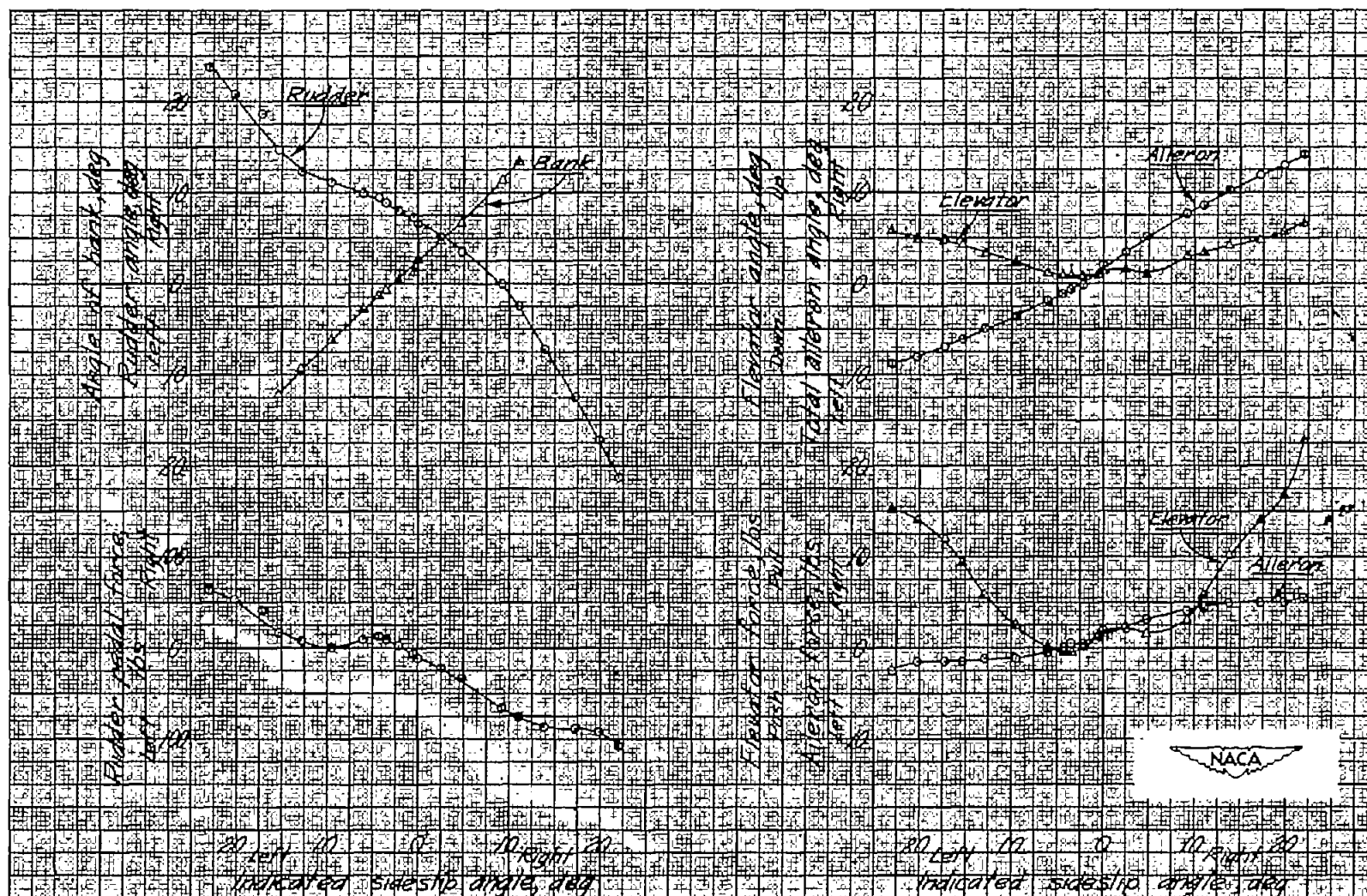
(a) 149-mile-per-hour calibrated airspeed at 23,000 feet average altitude.

Figure 14.- Directional stability and control characteristics of the F-47D-30 in the glide condition at high altitude.



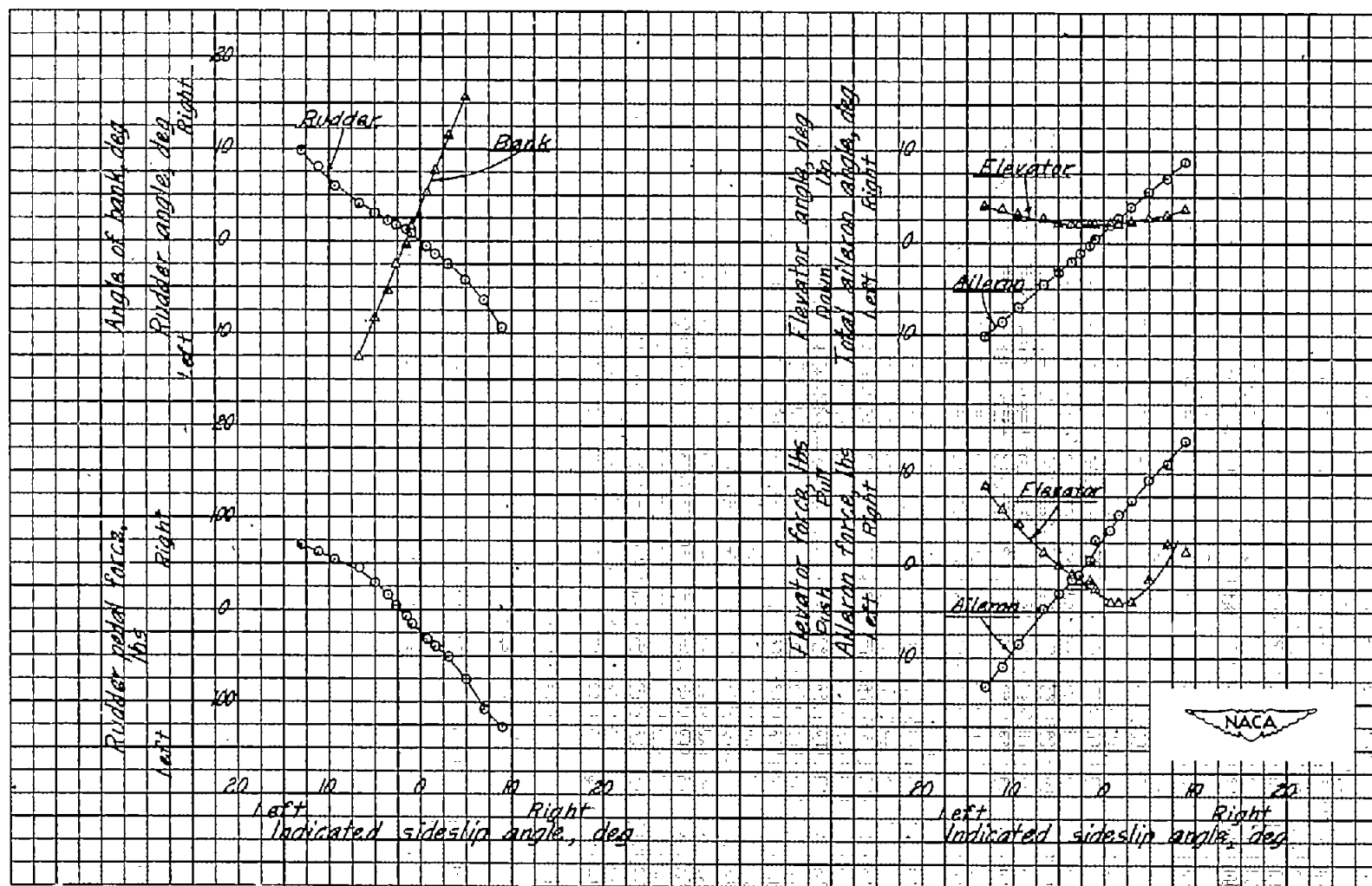
(b) 270-mile-per-hour calibrated airspeed at 22,000 feet average altitude.
 Data obtained by the continuous-sideslip method.

Figure 14.- Concluded.



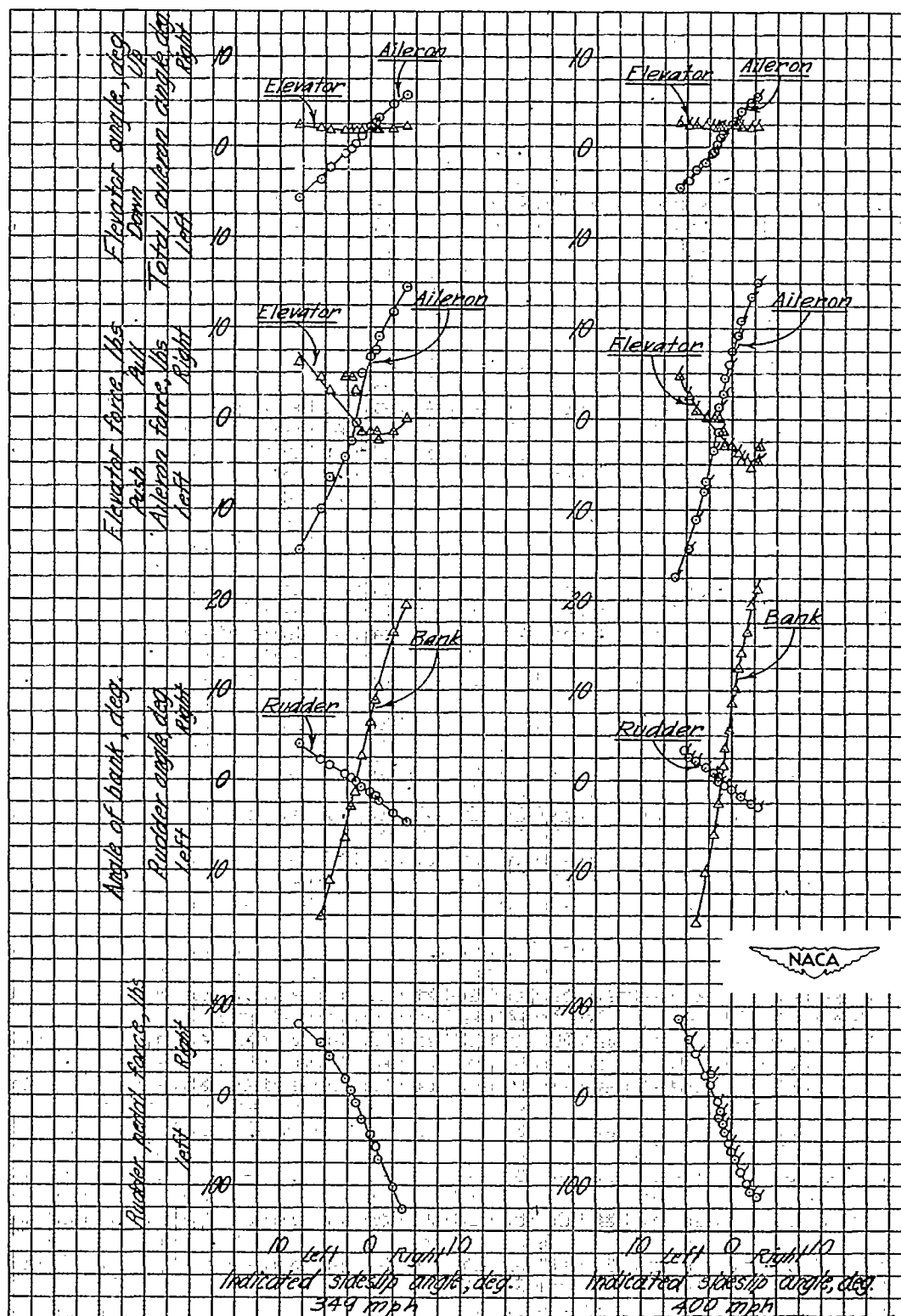
(a) 149-mile-per-hour calibrated airspeed at 5000 feet average altitude.

Figure 15.- Directional stability and control characteristics of the F-47D-30 airplane in the power-on clean condition at low altitude.



(b) 271-mile-per-hour calibrated airspeed at 5000 feet altitude.

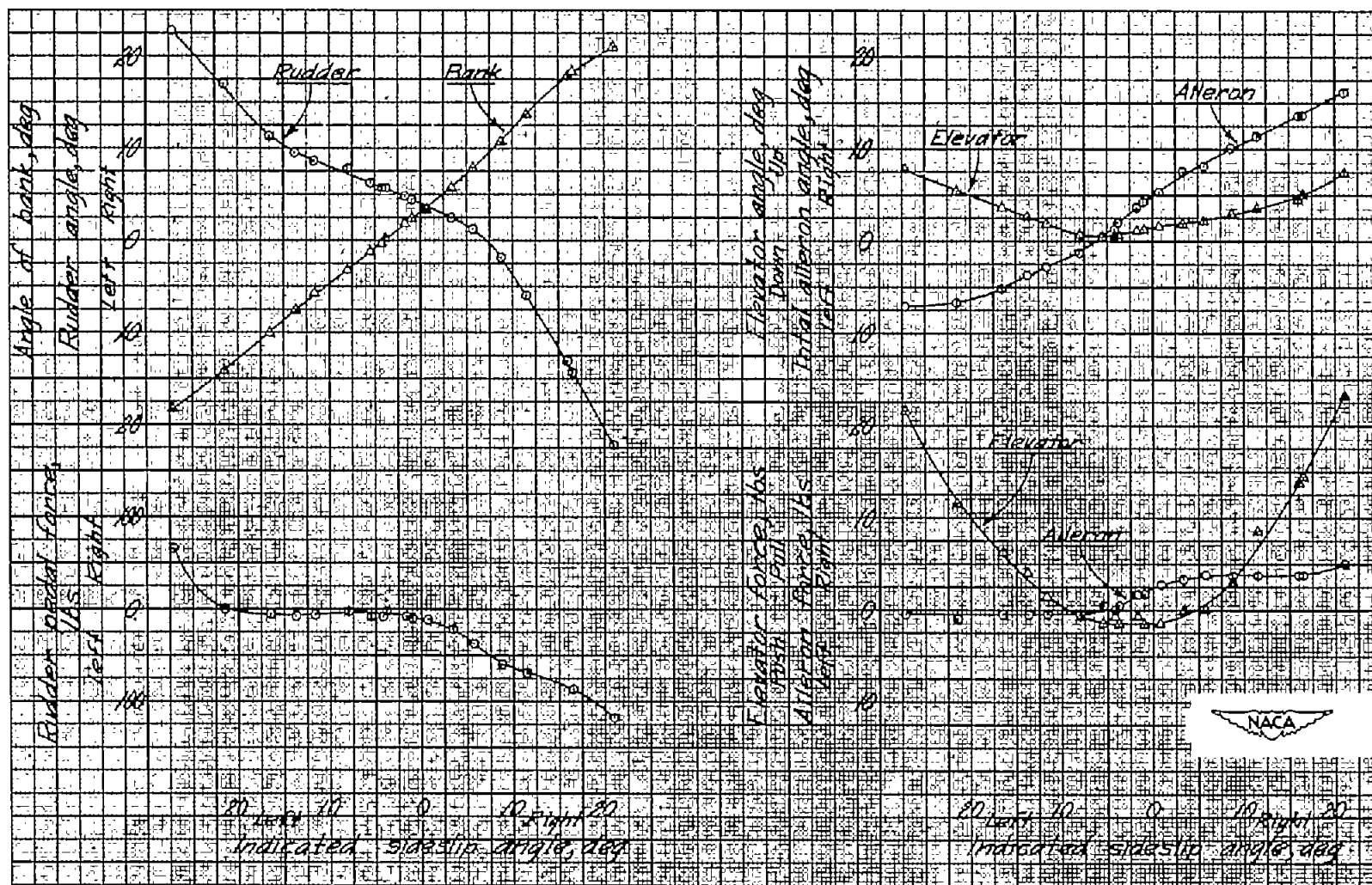
Figure 15.- Continued.



(c) 349-mile-per-hour calibrated
 airspeed at 5000 feet average
 altitude.

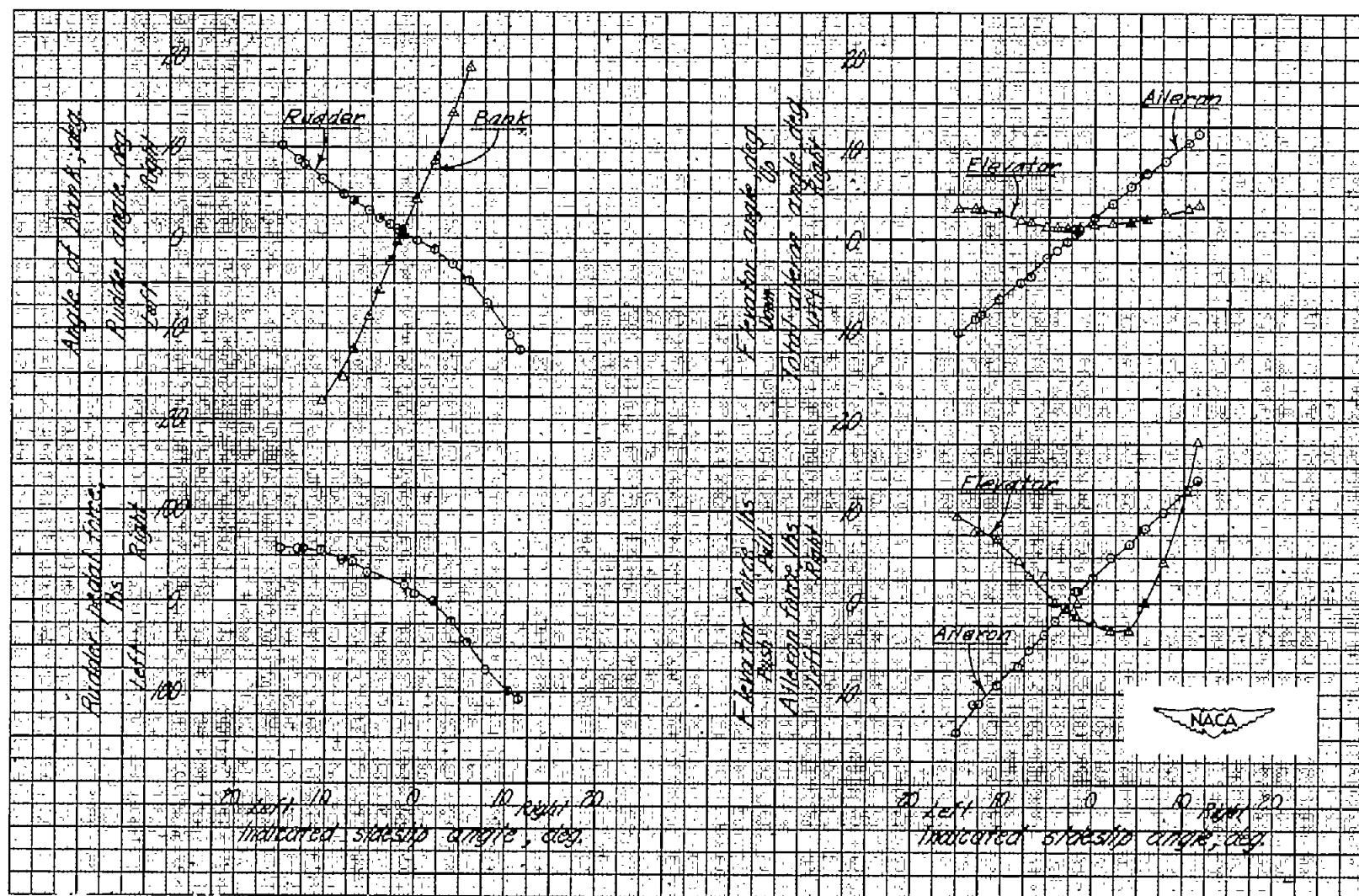
(d) 400-mile-per-hour calibrated
 airspeed at 5000 feet average
 altitude. Data obtained by the
 continuous-sideslip method.

Figure 15.- Concluded.



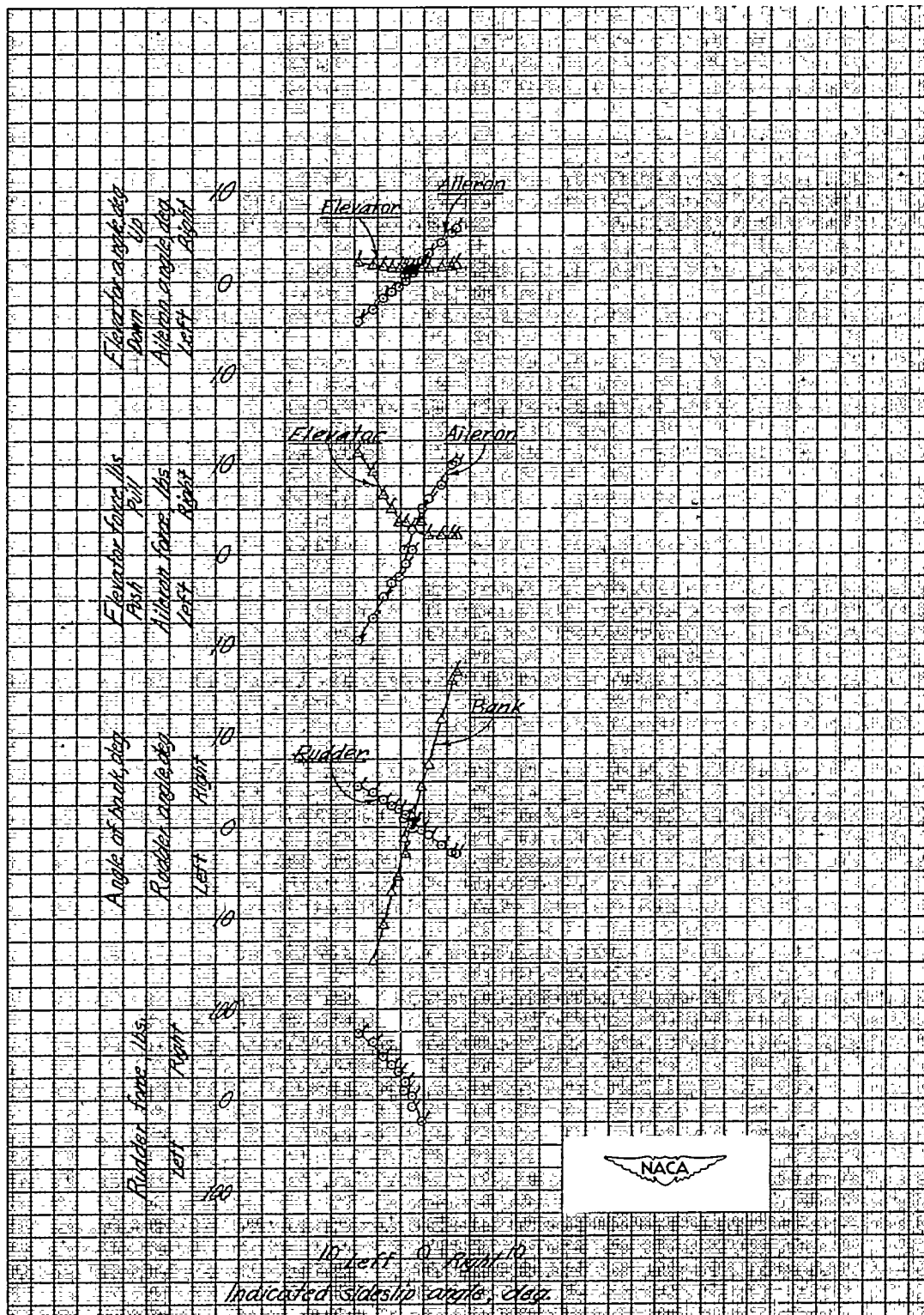
(a) 149-mile-per-hour calibrated airspeed at 27,000 feet average altitude.

Figure 16.- Directional stability and control characteristics in the power-on clean condition at high altitude.



(b) 269-mile-per-hour calibrated airspeed at 25,000 feet average altitude.

Figure 16.- Continued.



(c) 324-mile-per-hour calibrated airspeed at 23,000 feet average altitude.
 Data obtained by the continuous-sideslip method.

Figure 16.- Concluded.

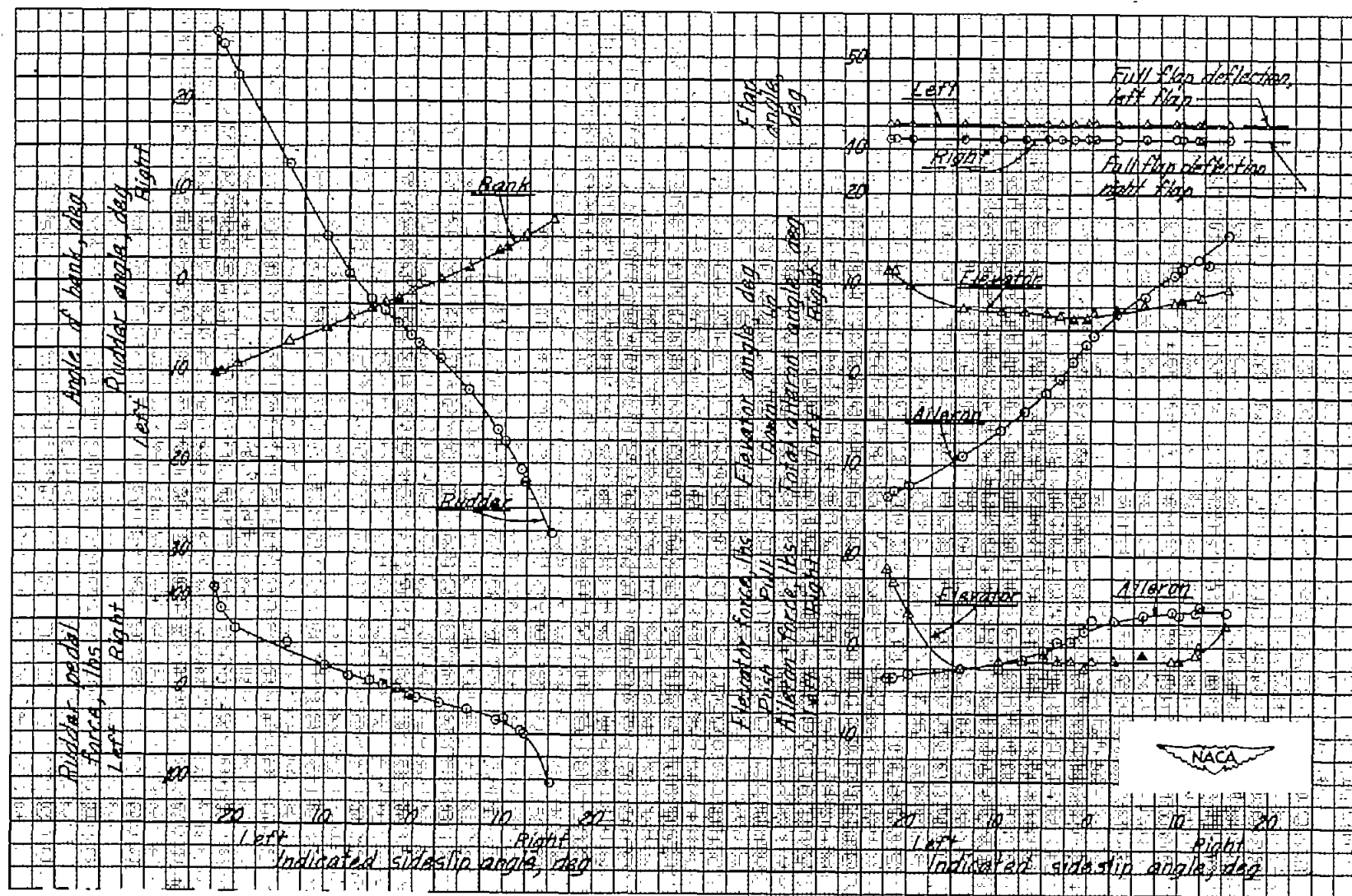
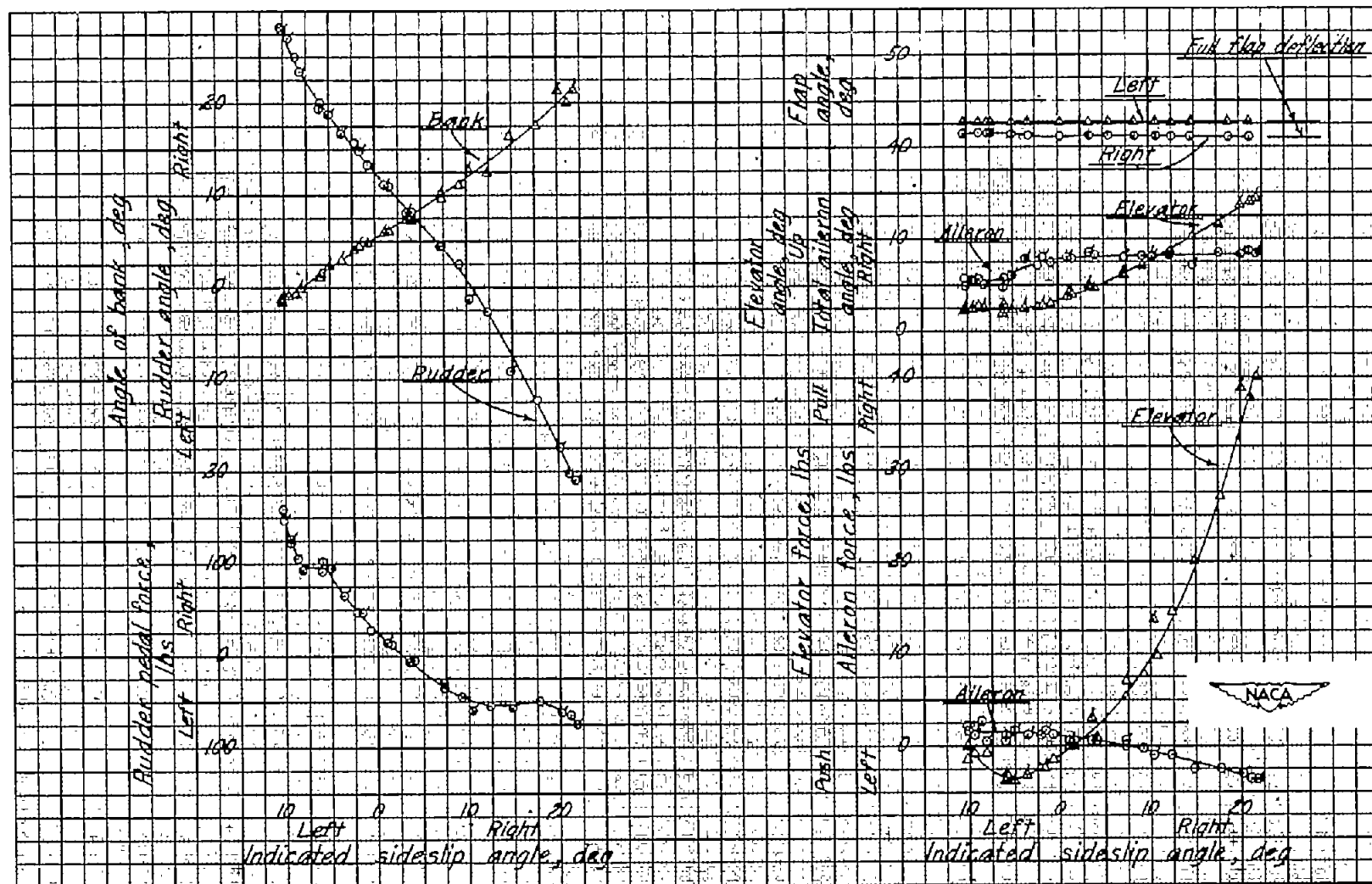
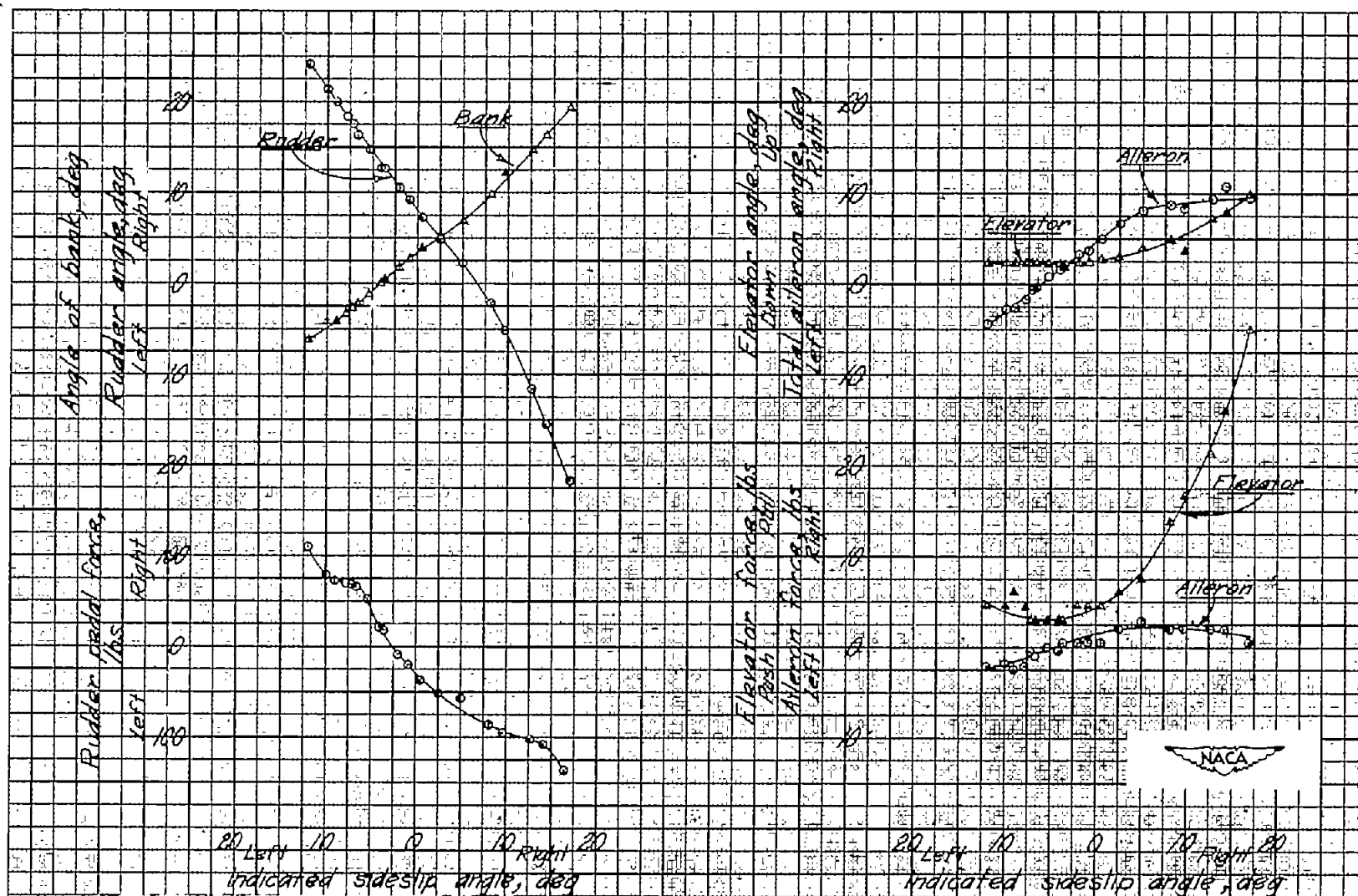


Figure 17.- Directional stability and control characteristics of the F-47D-30 airplane at 118 miles per hour. Landing condition at 5000 feet average altitude.



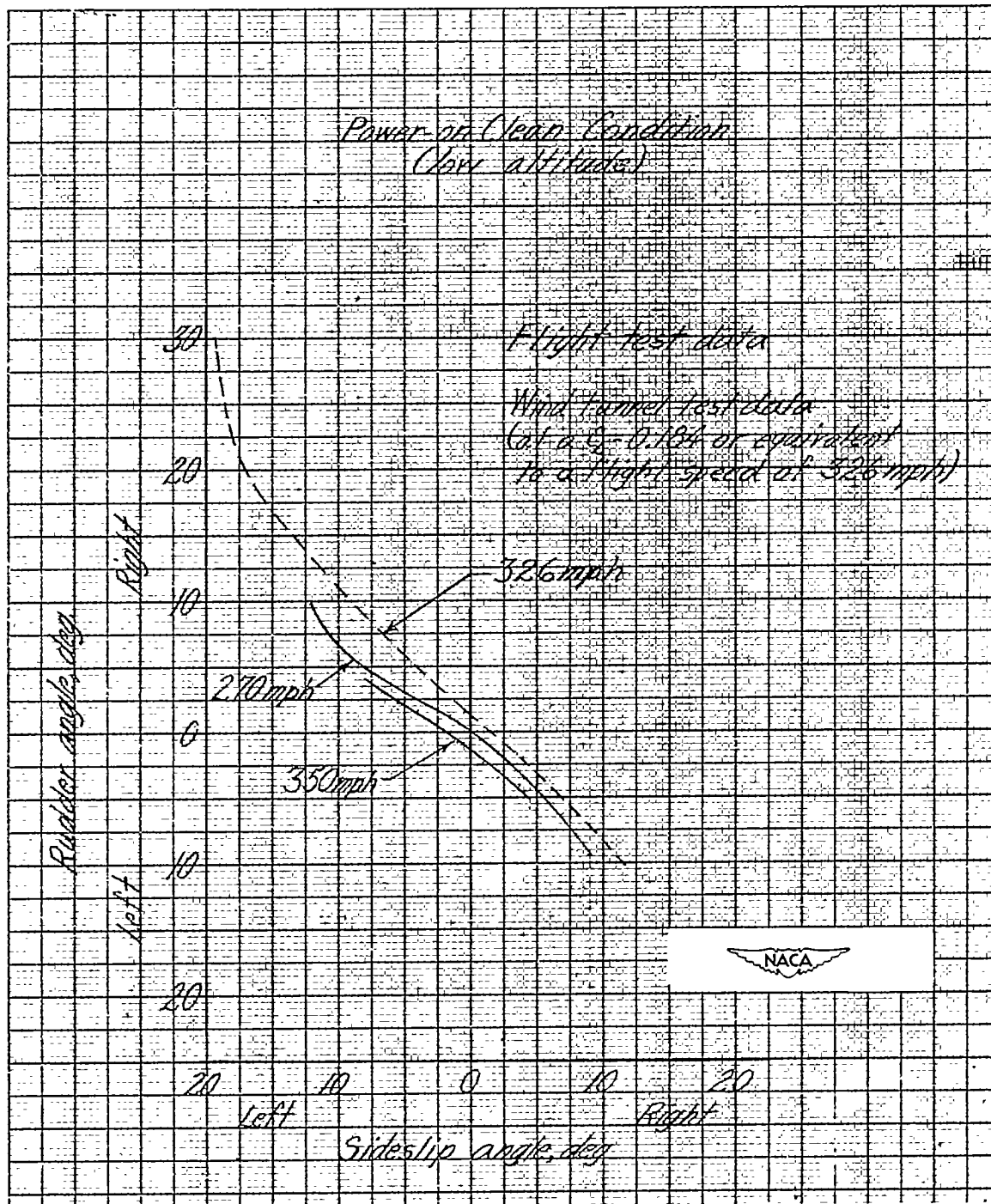
(a) 103 miles per hour. Flagged symbols indicate data obtained by the continuous-sideslip method.

Figure 18.- Directional stability and control characteristics of the F-47D-30 airplane. Wave-off condition at 5000 feet average altitude.



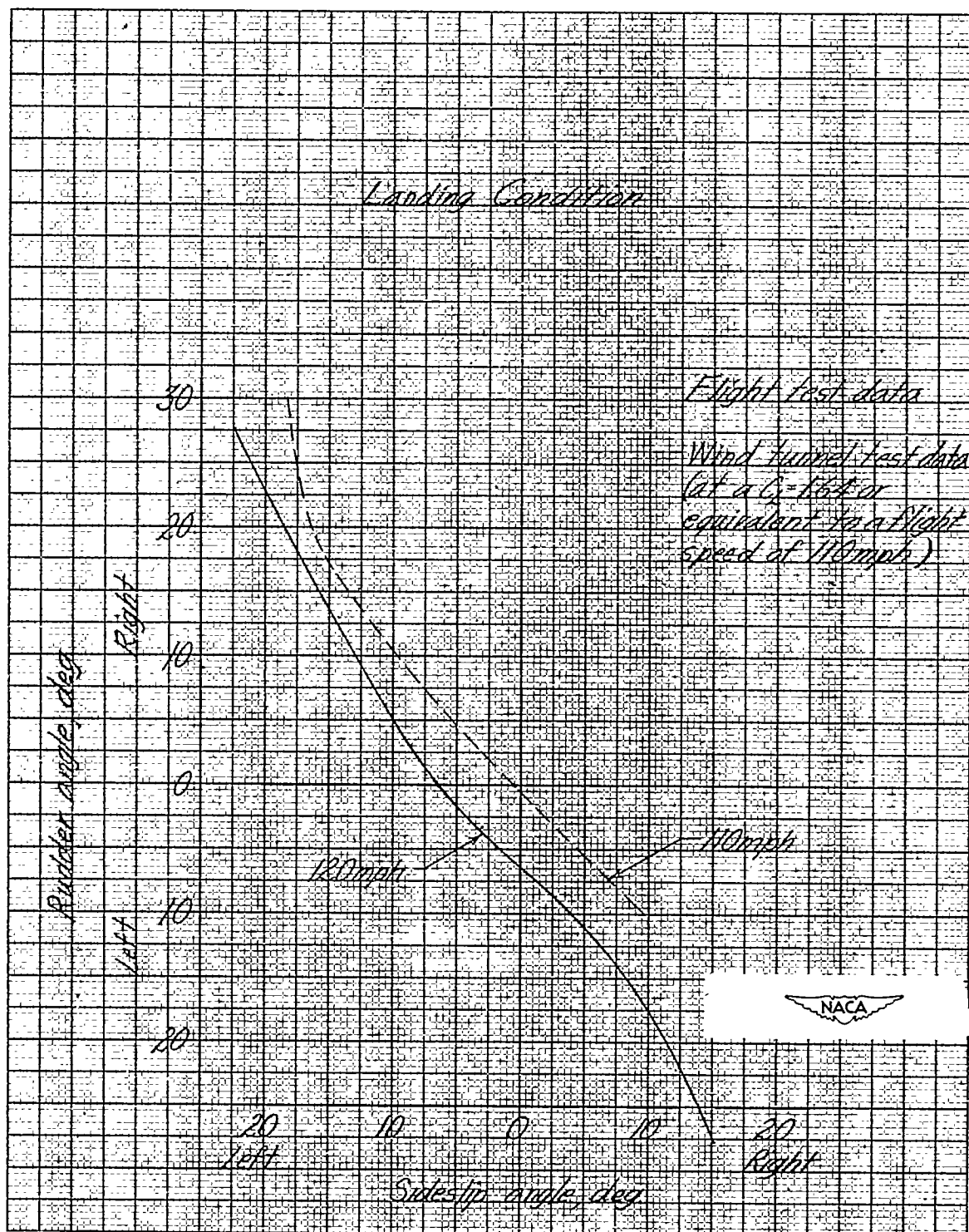
(b) 123 miles per hour.

Figure 18.- Concluded.



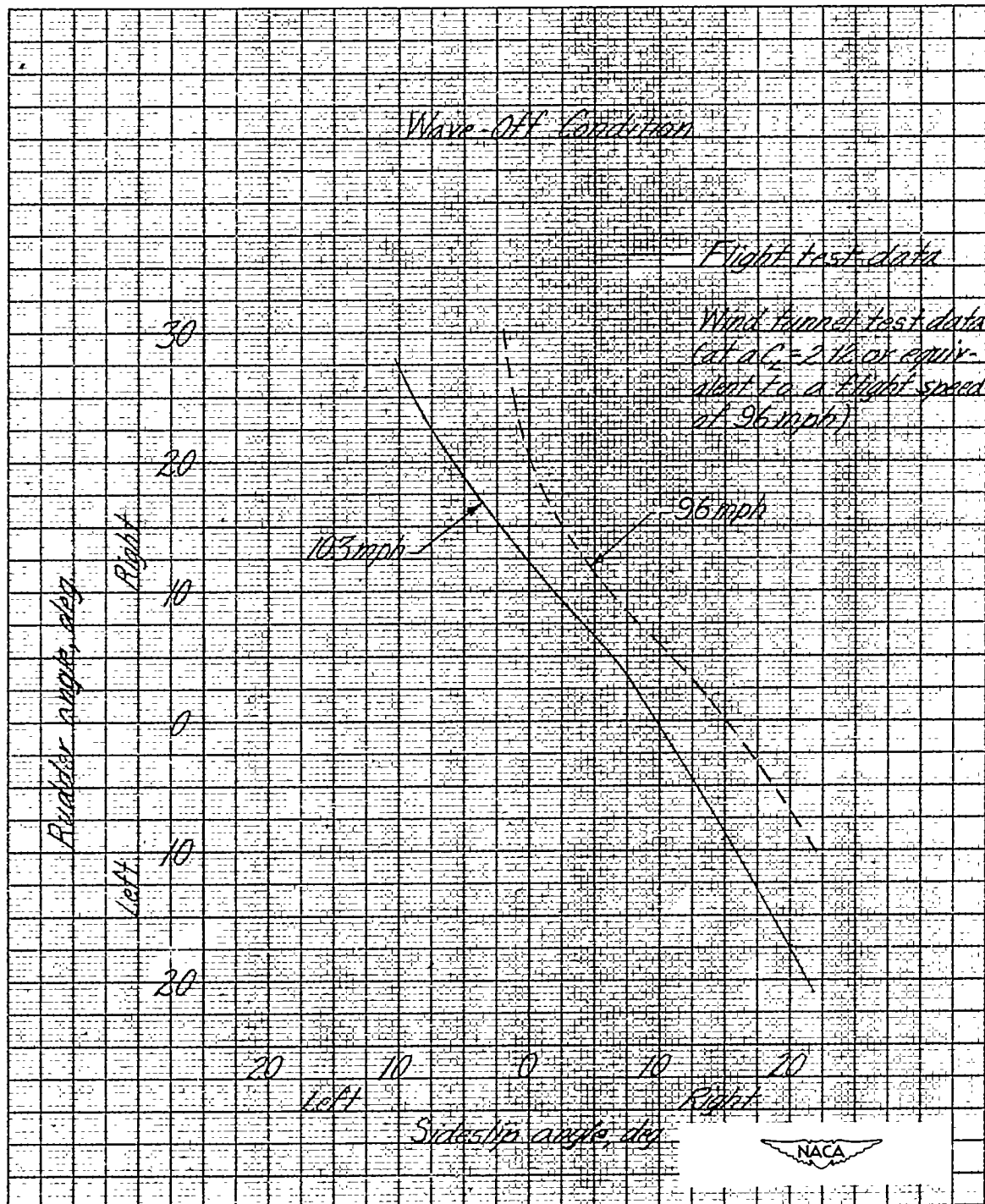
(a) Power-on, clean, low-altitude condition.

Figure 19.- Comparison of wind-tunnel and flight test data of the F-47D-30 airplane.



(b) Landing condition.

Figure 19.- Continued.



(c) Wave-off condition.

Figure 19.- Concluded.

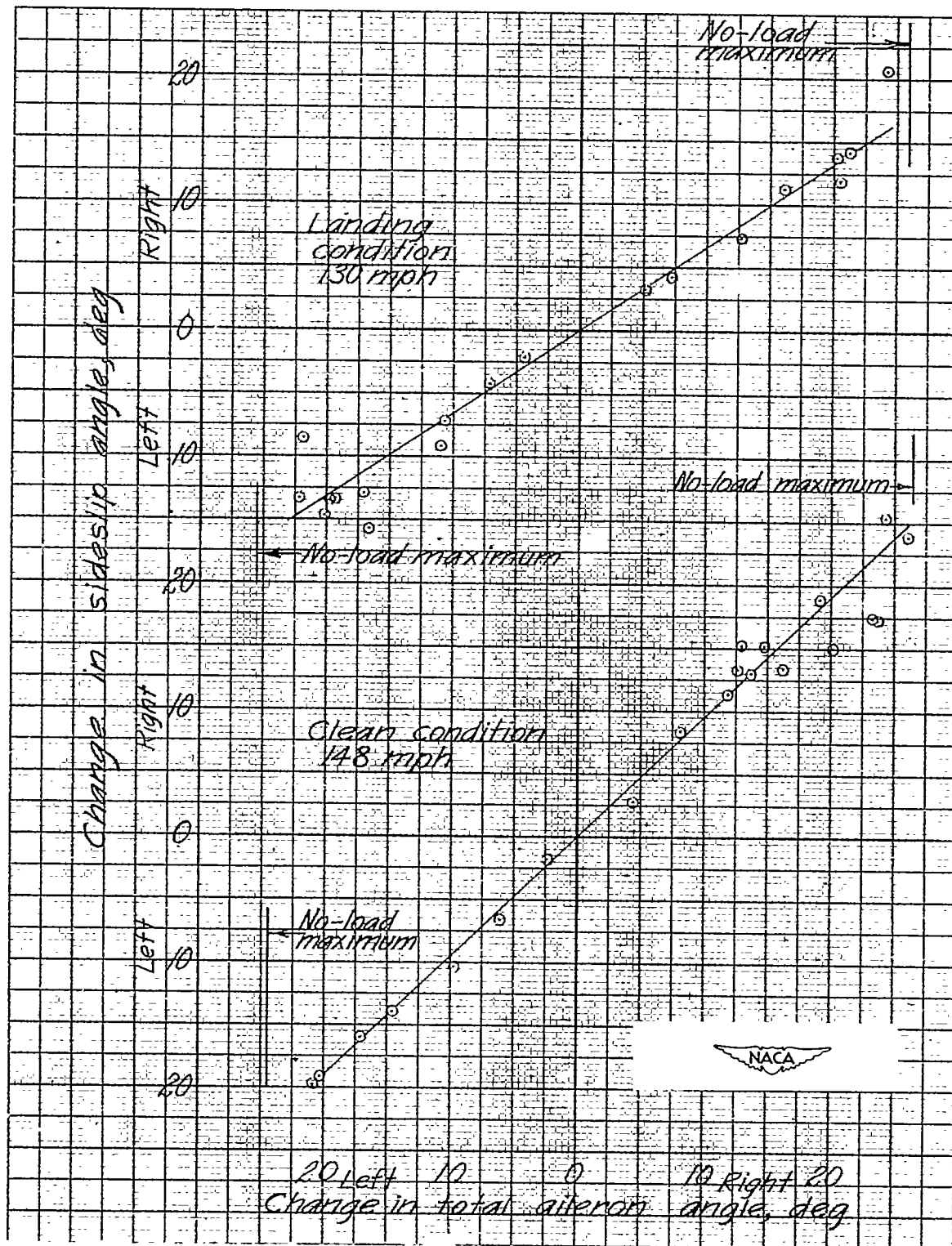


Figure 20.- Maximum change in sideslip attained during abrupt aileron rolls out of 45° banked turns with rudder fixed. Power for level flight.

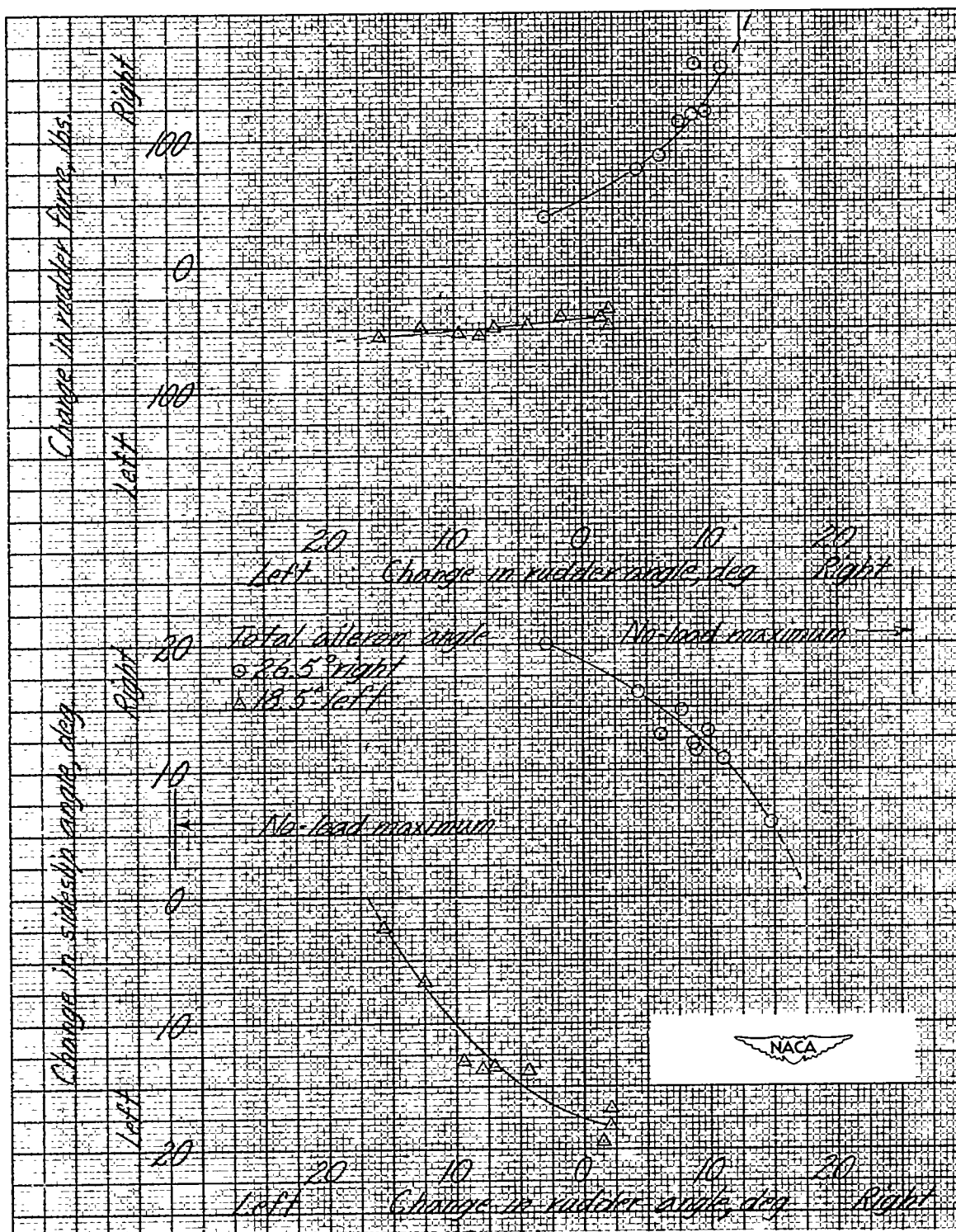
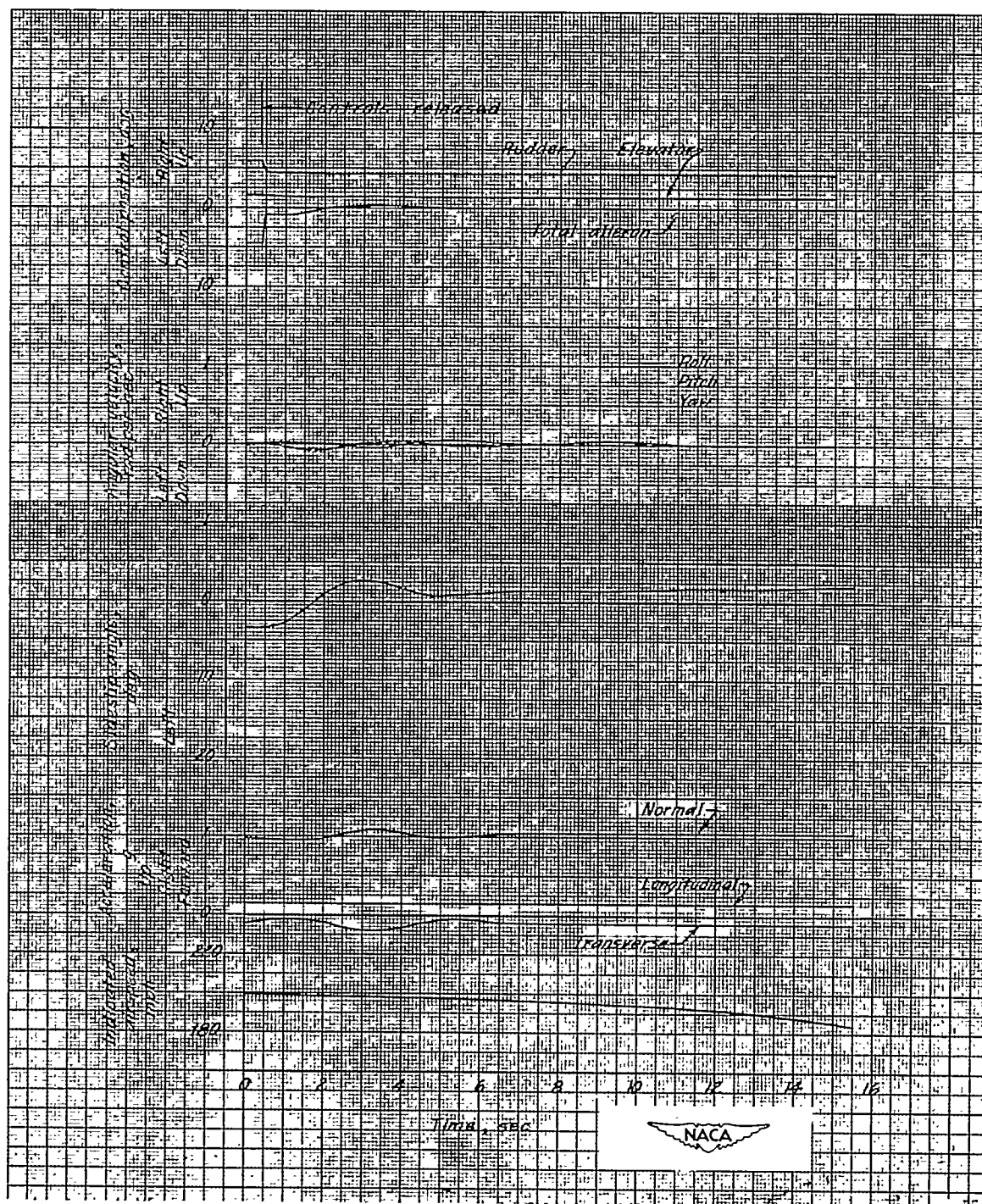
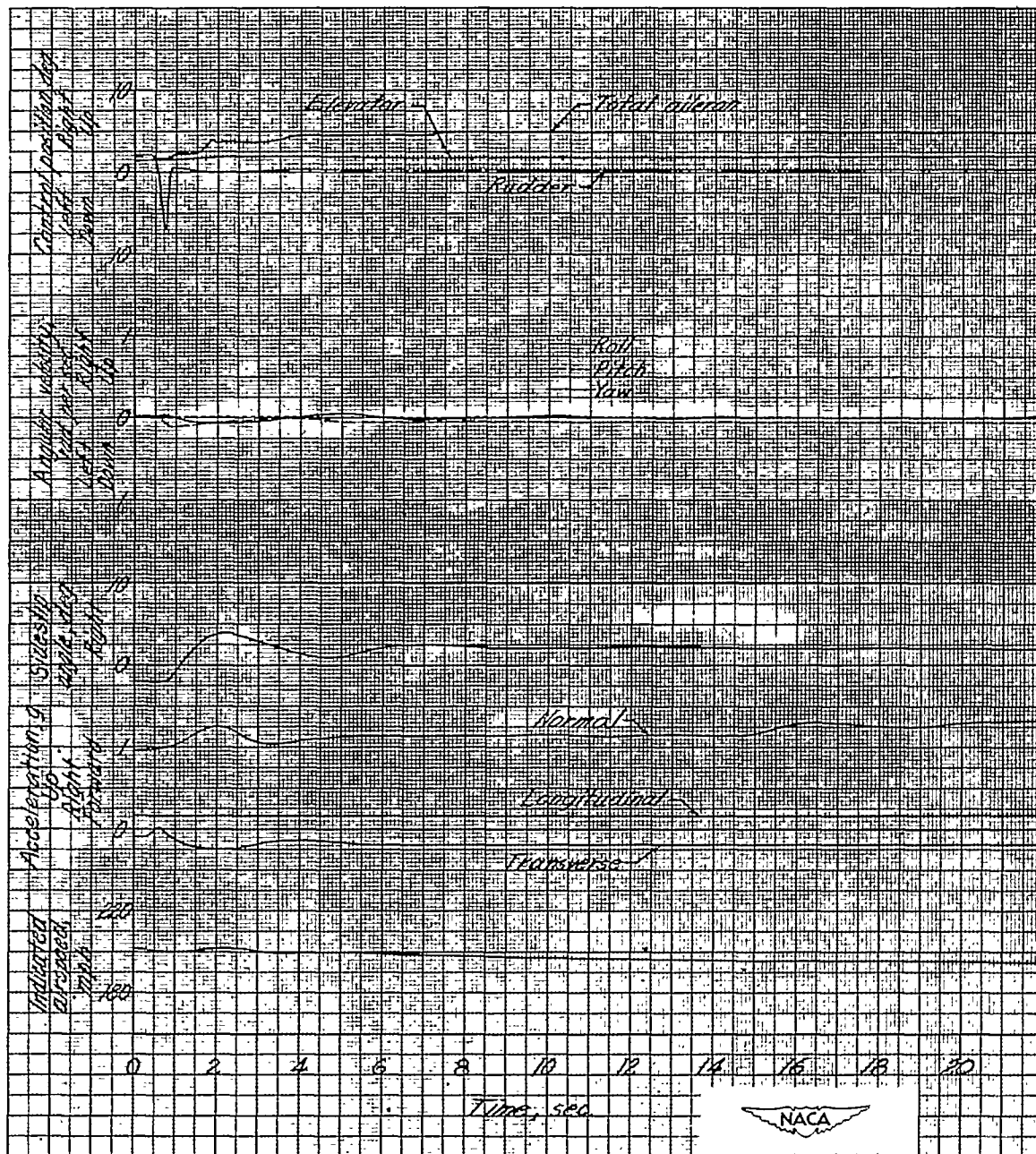


Figure 21.- Maximum change in sideslip and rudder force attained during abrupt aileron rolls out of 45° banked turns with varying amounts of rudder deflection. Clean condition; power for level flight at 148-mile-per-hour calibrated airspeed.



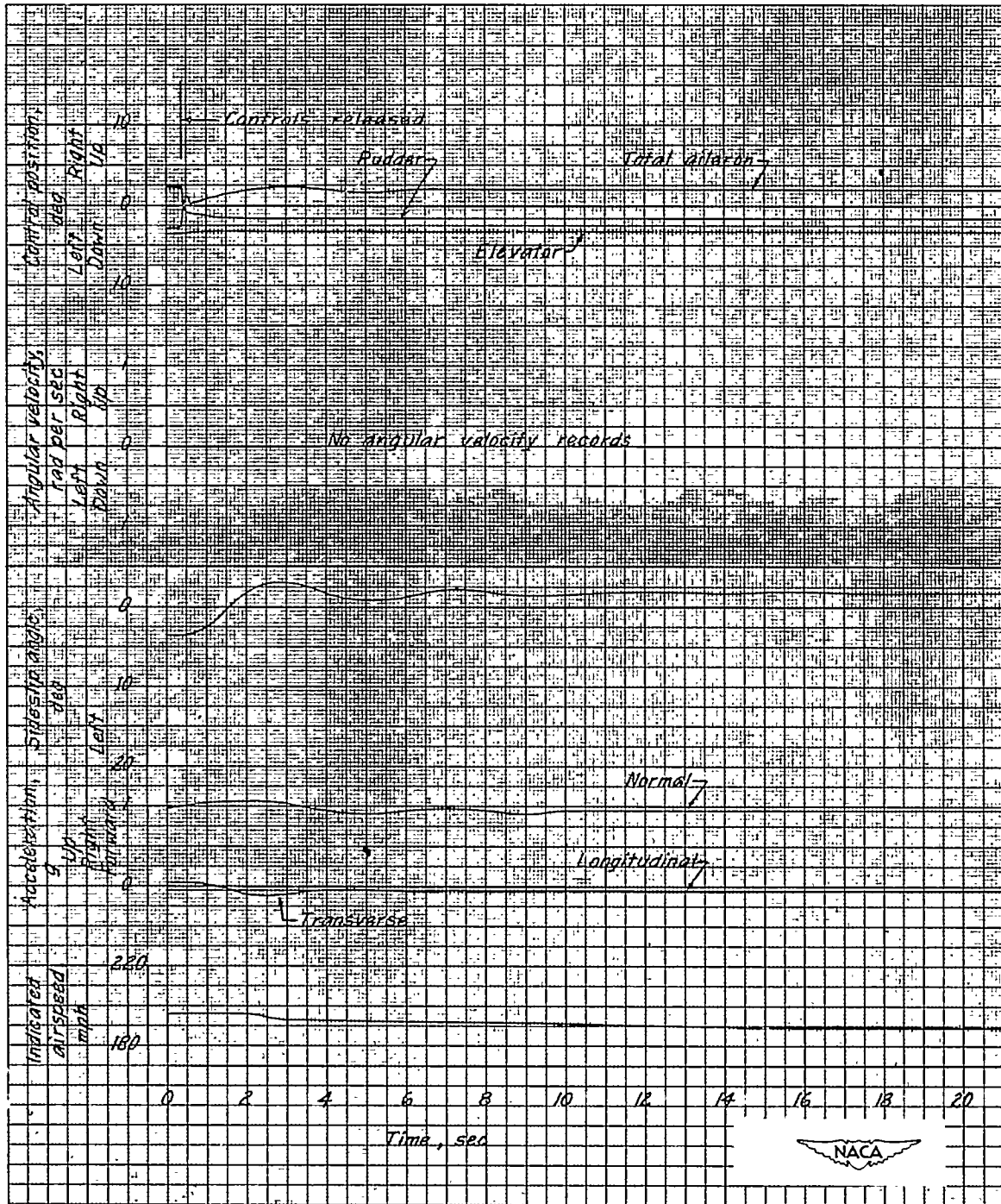
(a) 5000 feet altitude. Oscillation started from a steady sideslip.

Figure 22.- Time history of a directional oscillation at 200 miles per hour. Power-on clean condition.



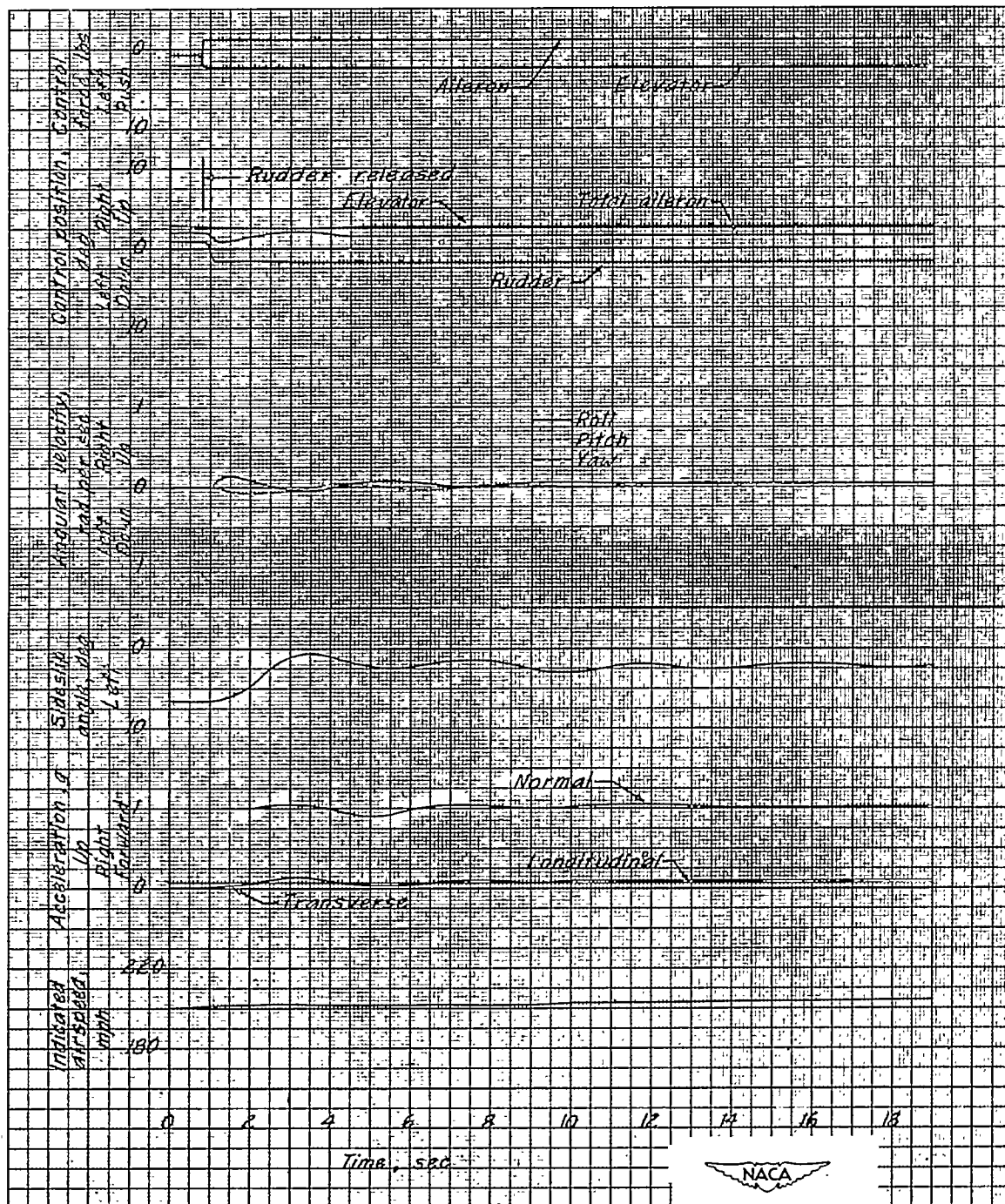
(b) 28,000 feet altitude. Oscillation started by a rudder kick. Airplane diverged spirally.

Figure 22.- Concluded.



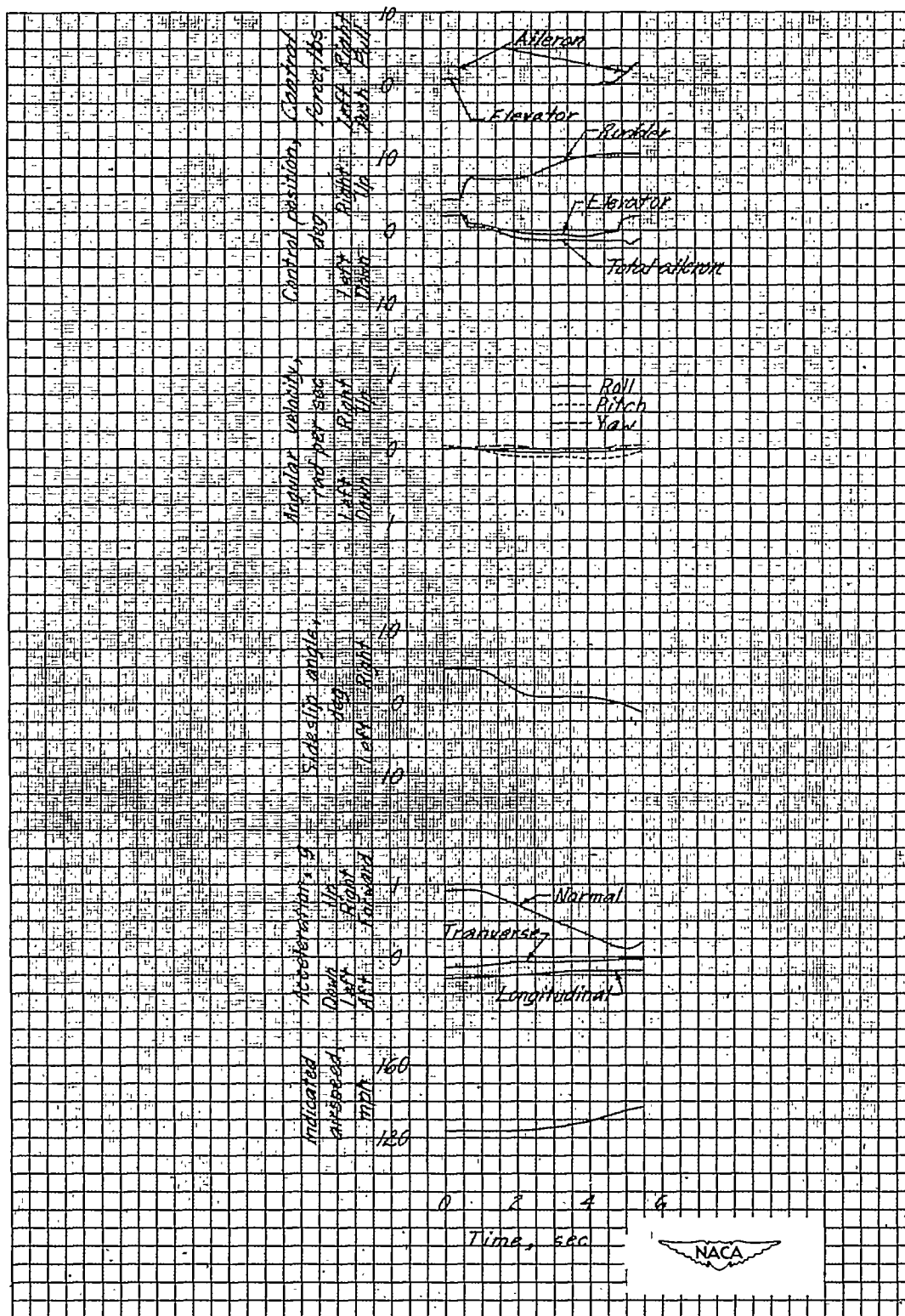
(a) 5000 feet altitude.

Figure 23.- Time history of a directional oscillation at 200 miles per hour started from a small angle of sideslip. Glide condition.



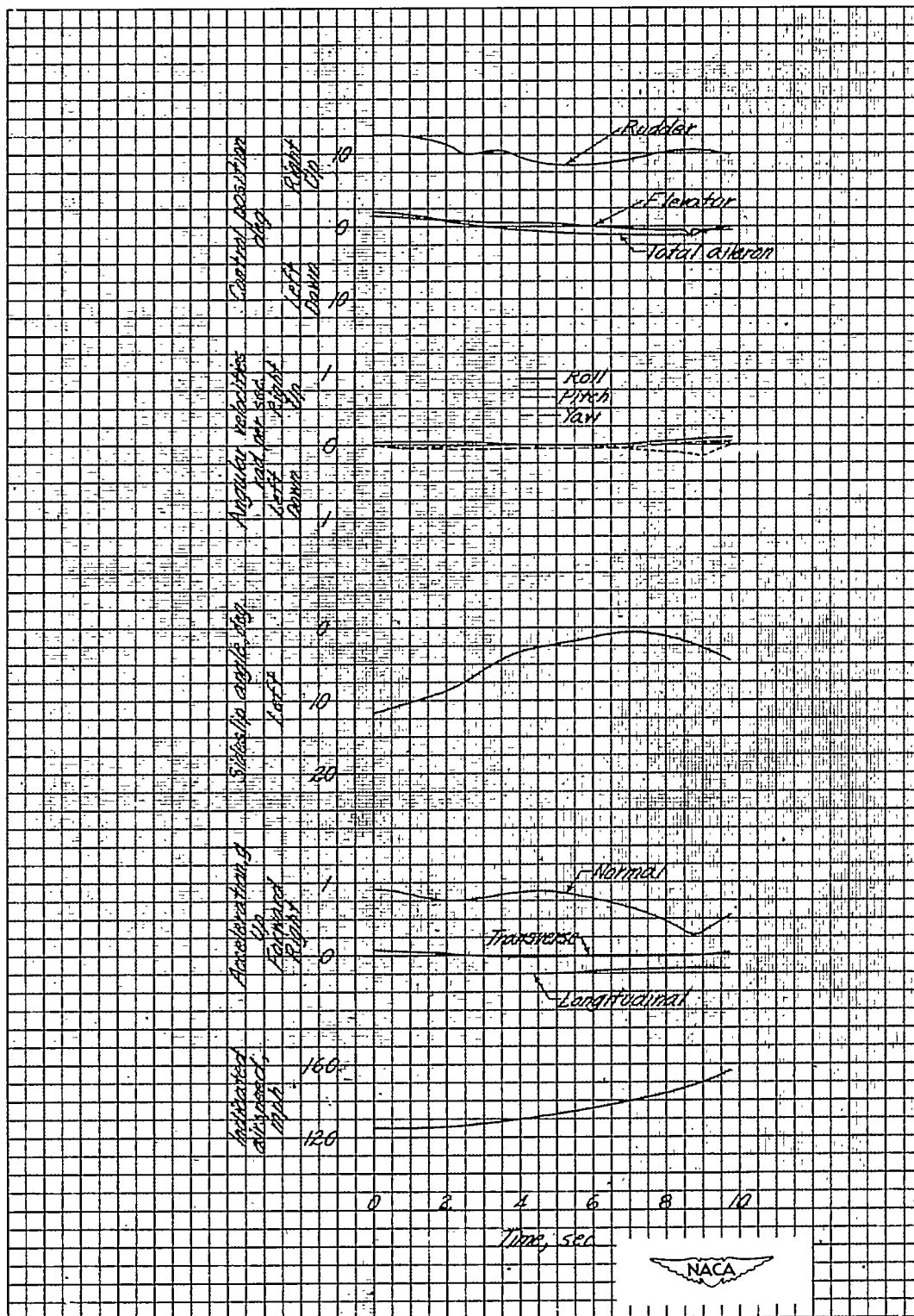
(b) 21,000 feet altitude. Elevator restrained to prevent longitudinal divergence.

Figure 23.- Concluded.



(a) Started from right sideslip and diverged rapidly nose down.

Figure 24.- Time history of a directional oscillation started from a steady sideslip at 125 miles per hour. Power-on clean condition.



(b) Started from left sideslip and diverged nose down. Controls were released before record started.

Figure 24.- Concluded.

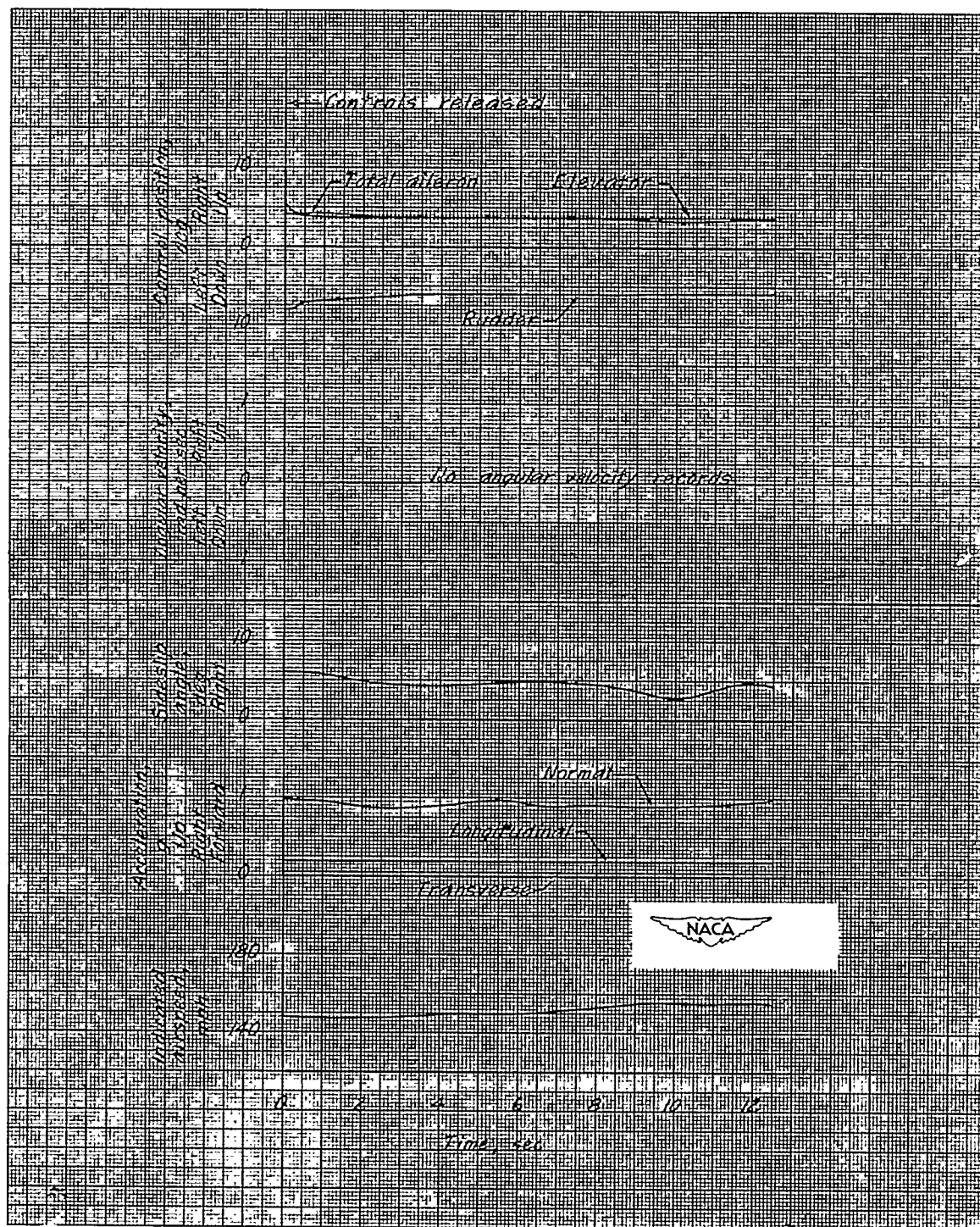


Figure 25.- Time history of an attempted directional oscillation started from a steady sideslip at 150 miles per hour. Landing condition.

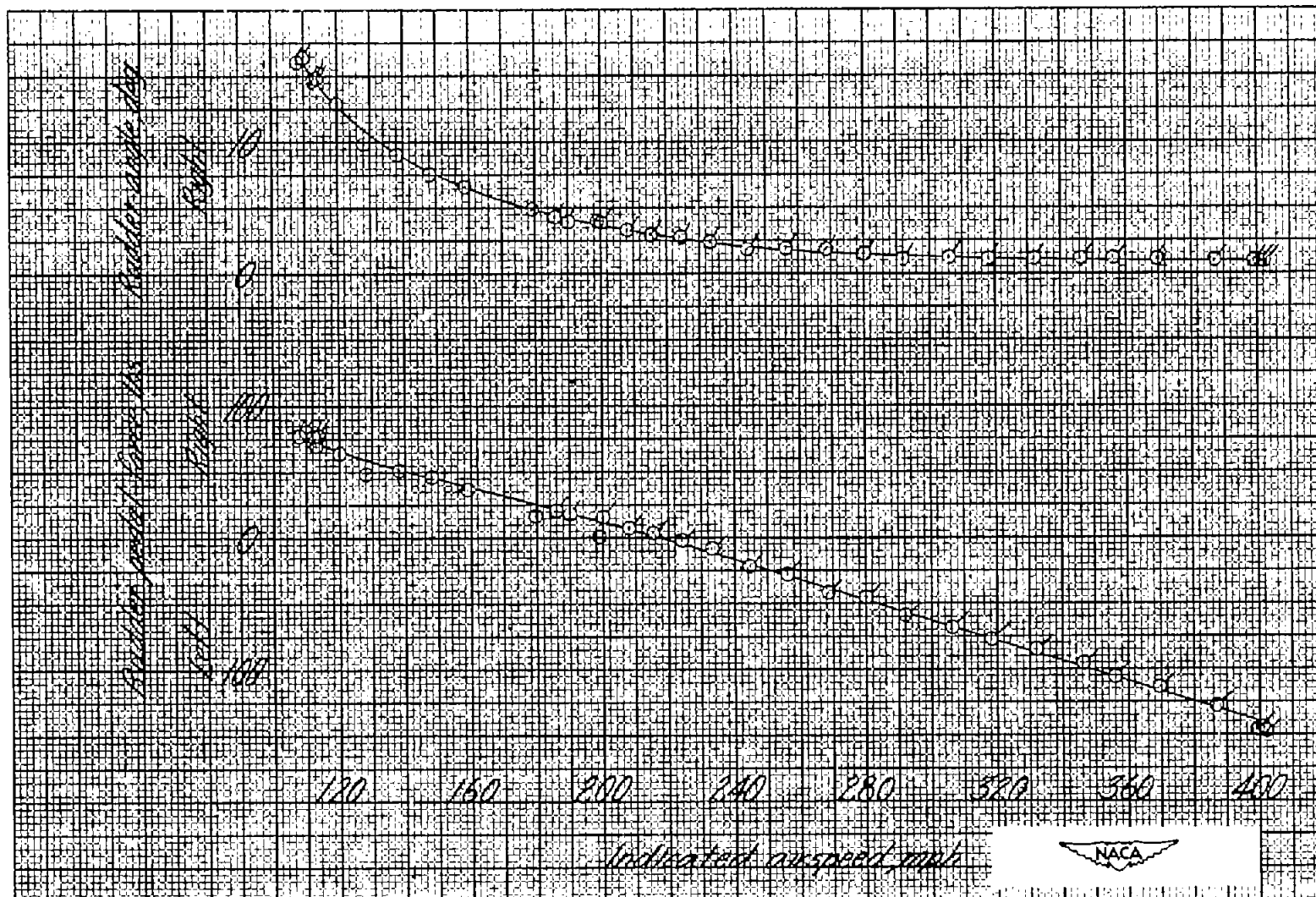
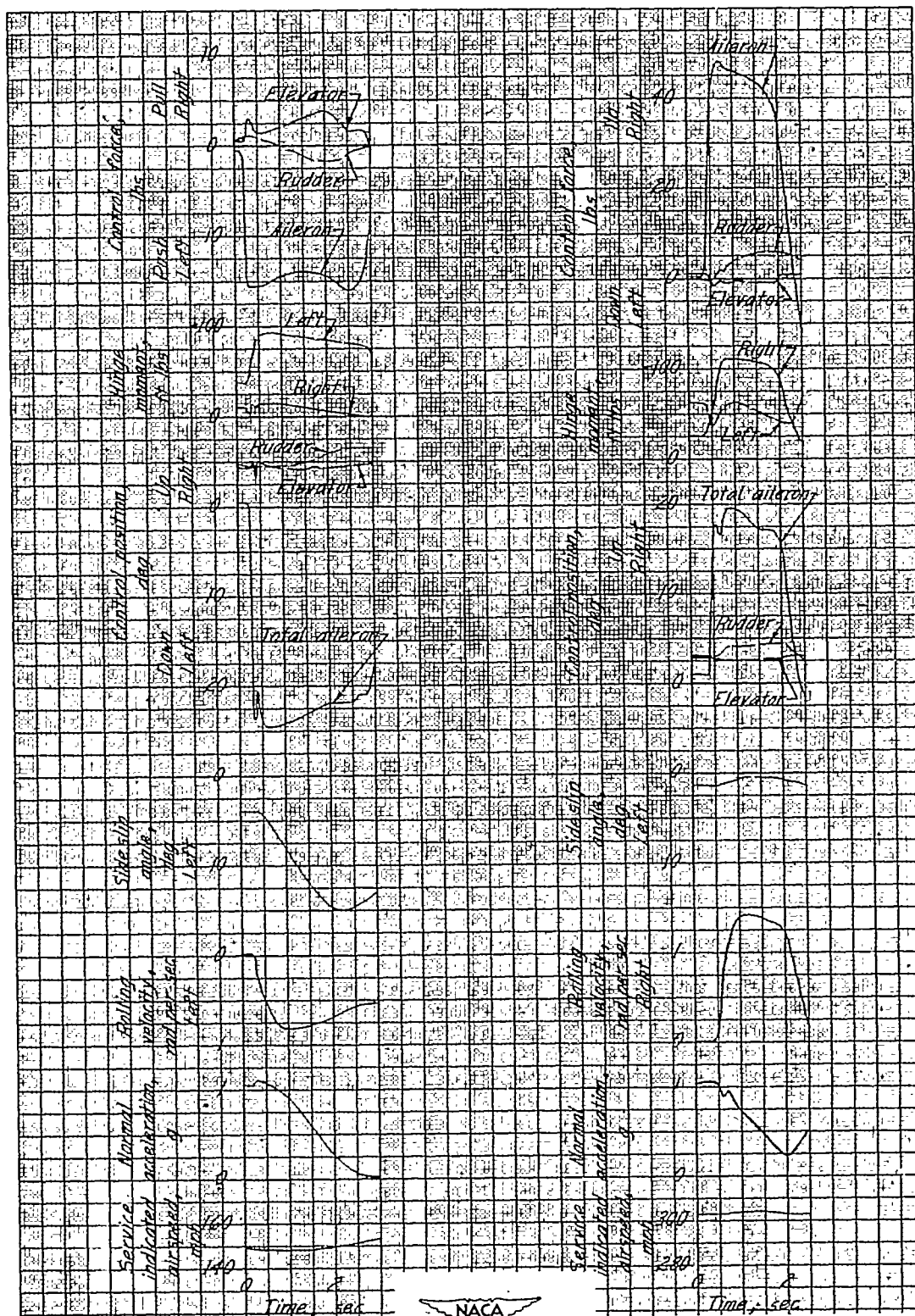


Figure 26.- The variation of rudder force and rudder angle with indicated airspeed in the power-on clean condition. F-47D-30 airplane.



(a) Left roll at 150 miles per hour. (b) Right roll at 300 miles per hour.

Figure 27.- Typical time histories of abrupt aileron rolls using partial aileron deflection, rudder fixed, clean condition, and normal rated power.

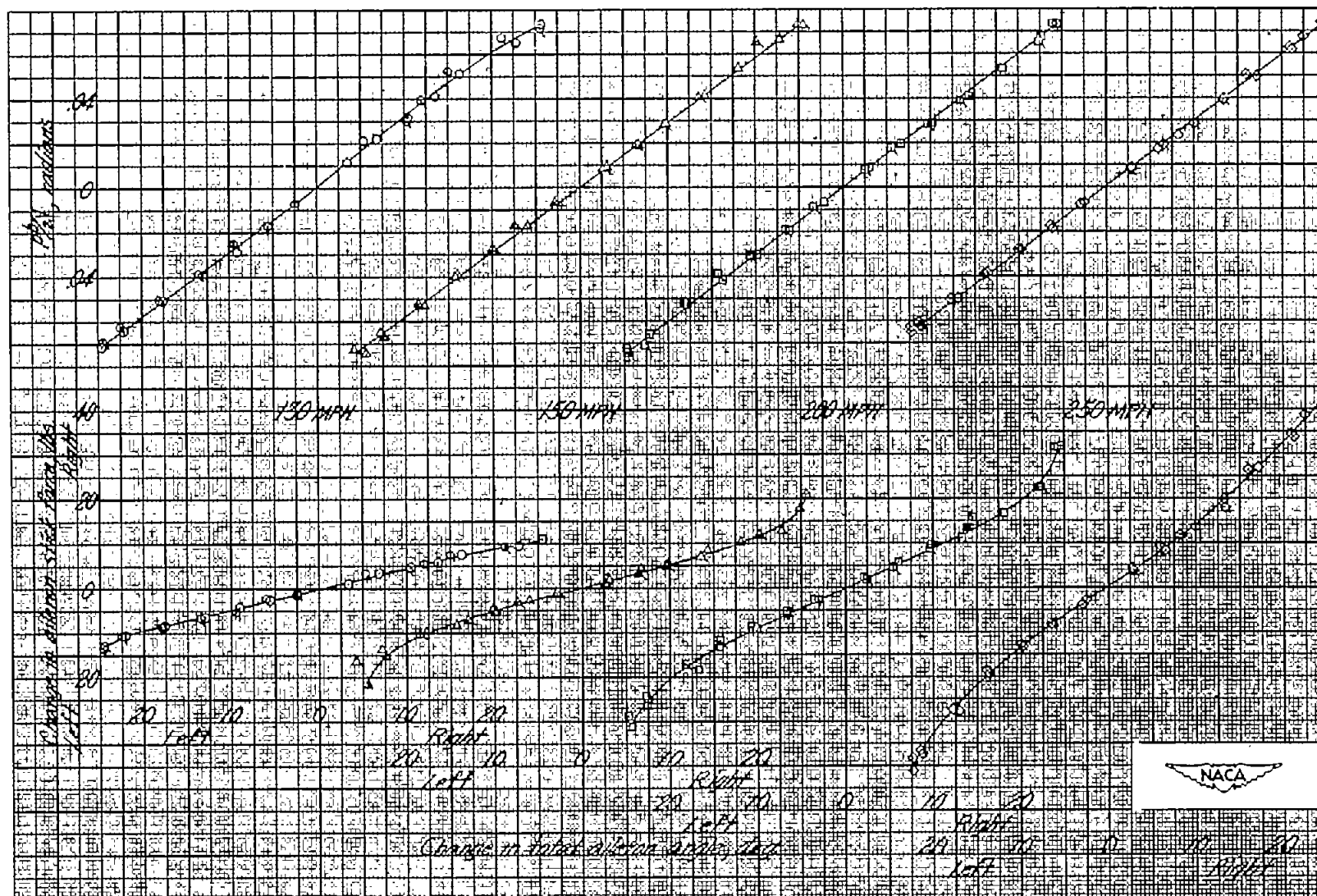


Figure 28.- Variation of helix angle $pb/2V$ and change in aileron stick force with change in total aileron angle. Average altitude 5000 feet; F-47D-30 airplane. (Different symbols indicate different flights.)

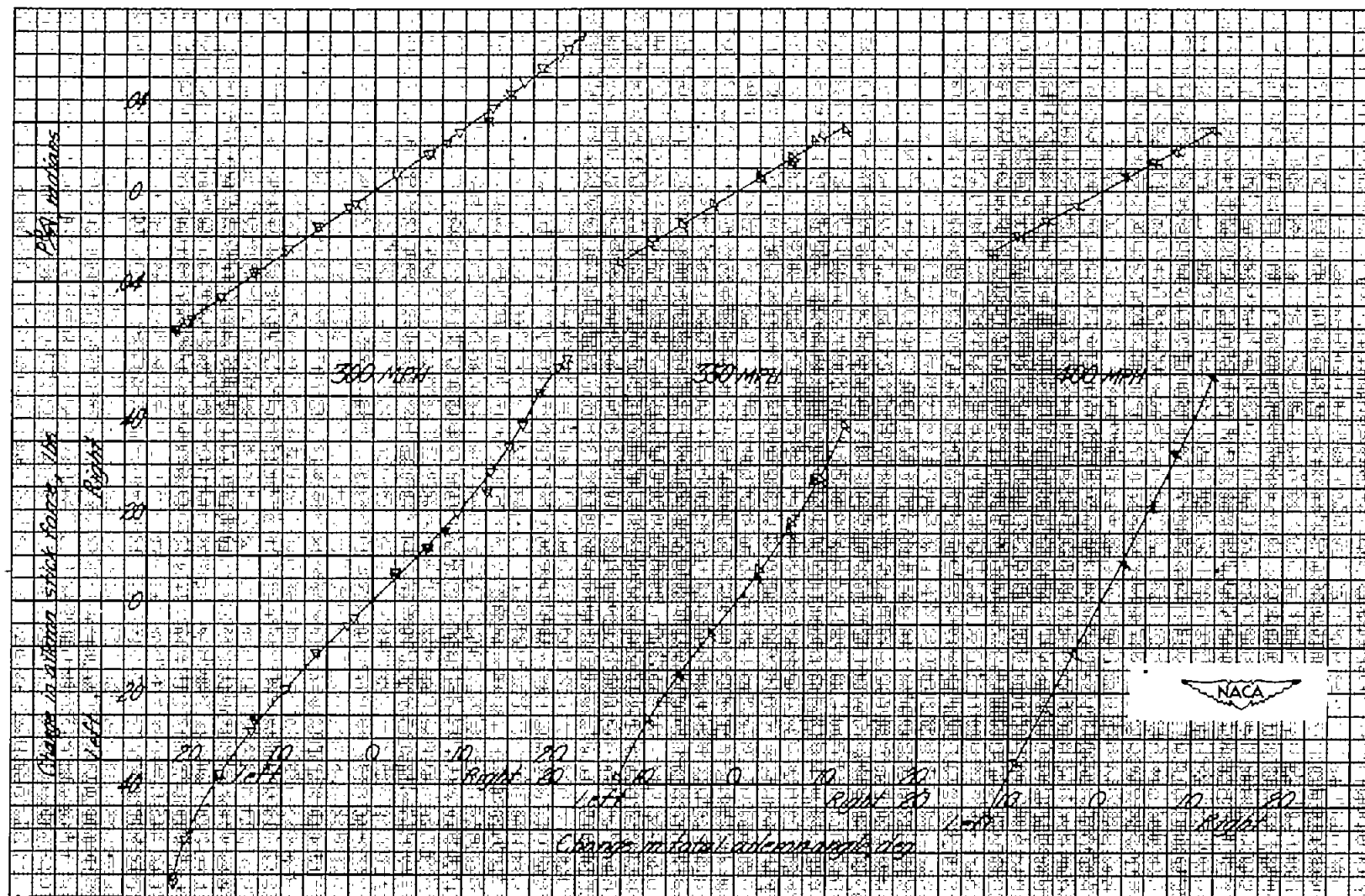


Figure 28.- Concluded.

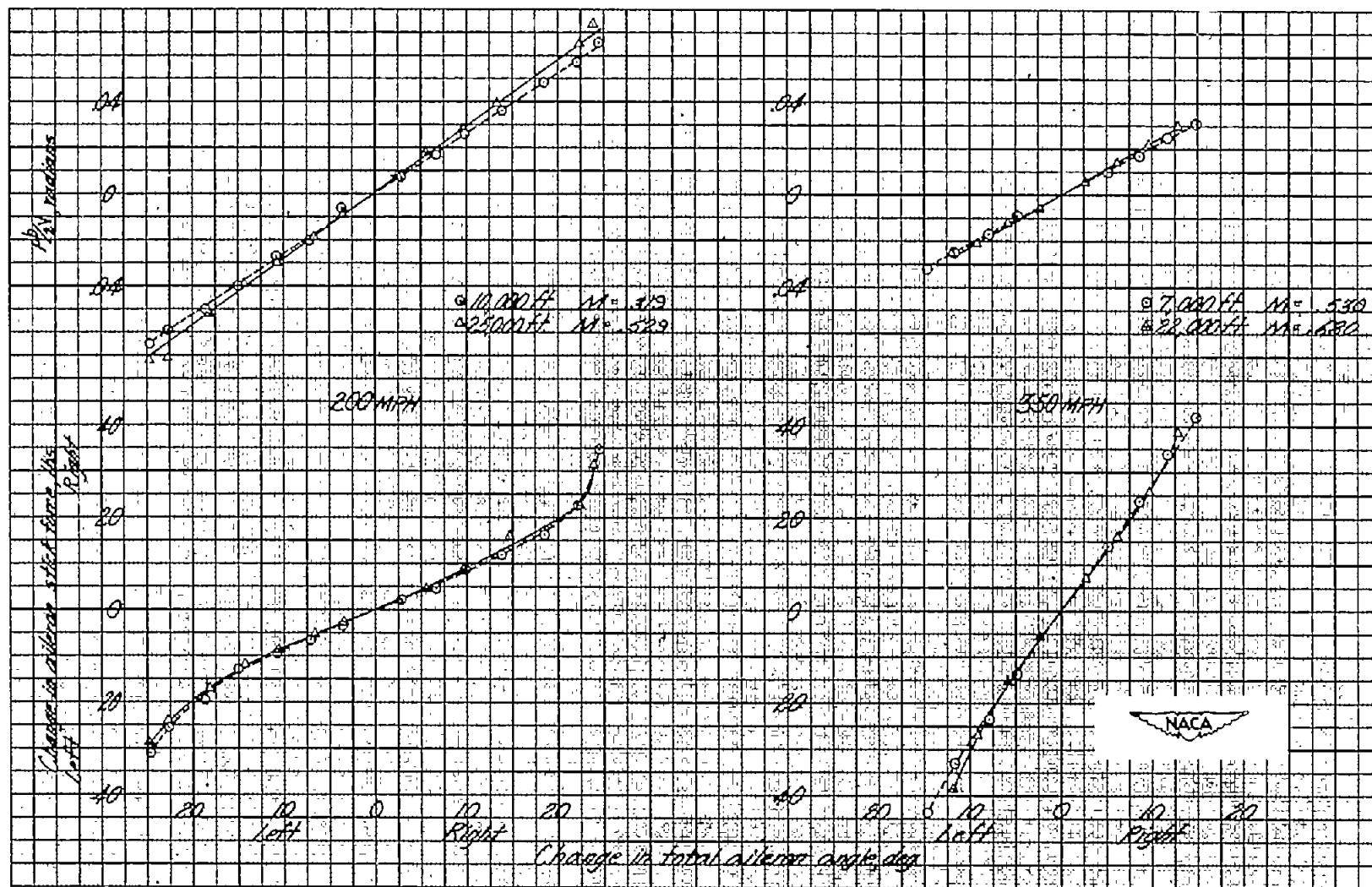


Figure 29.- Effect of altitude on variation of helix angle $pb/2V$ and change in aileron stick force with change in total aileron angle at 200 miles per hour and 350 miles per hour. F-47D-30 airplane.

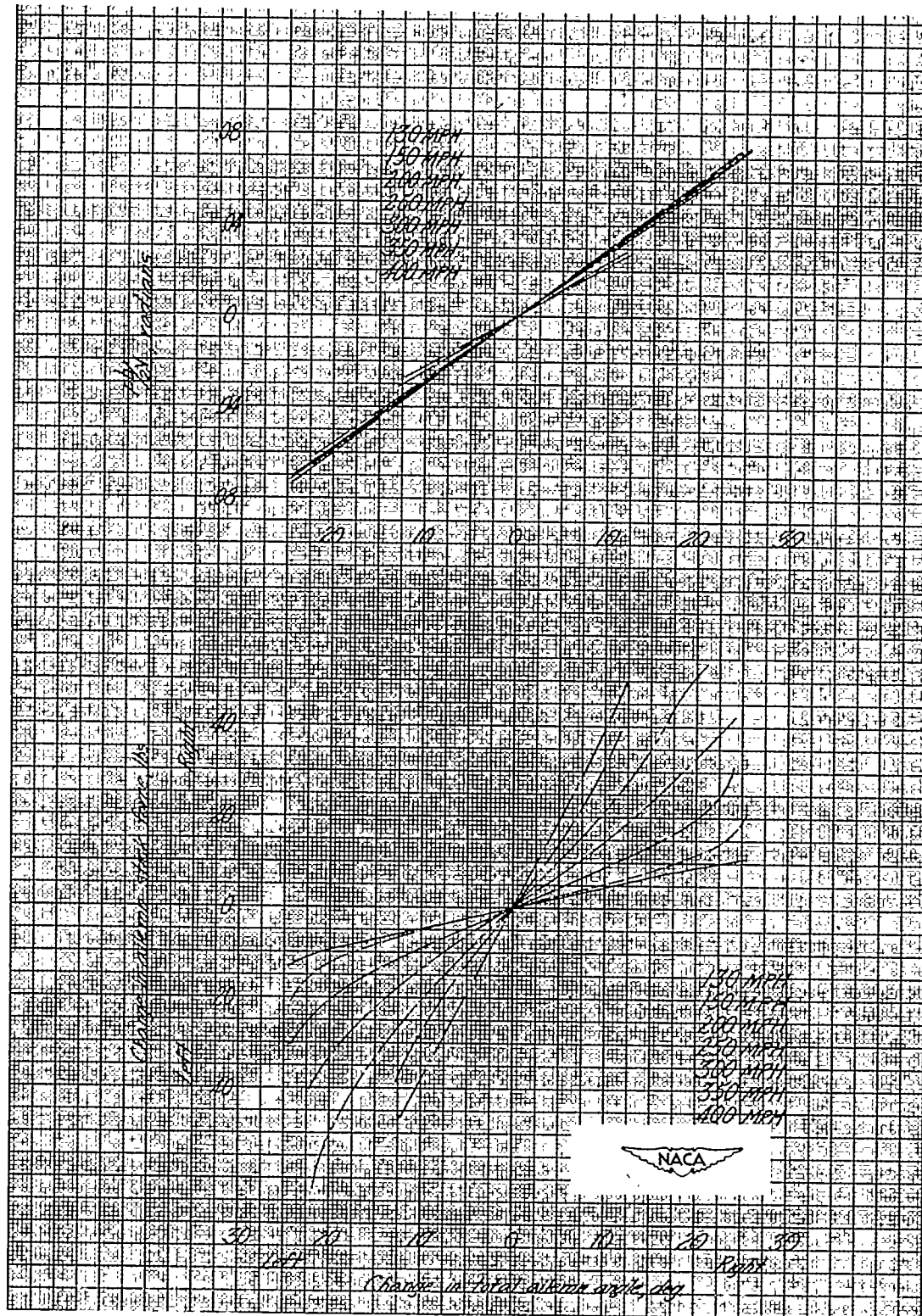


Figure 30.- Summary sheet showing variation of helix angle $pb/2V$ and change in aileron stick force with change in total aileron angle at various speeds. Average altitude of 5000 feet; F-47D-30 airplane.

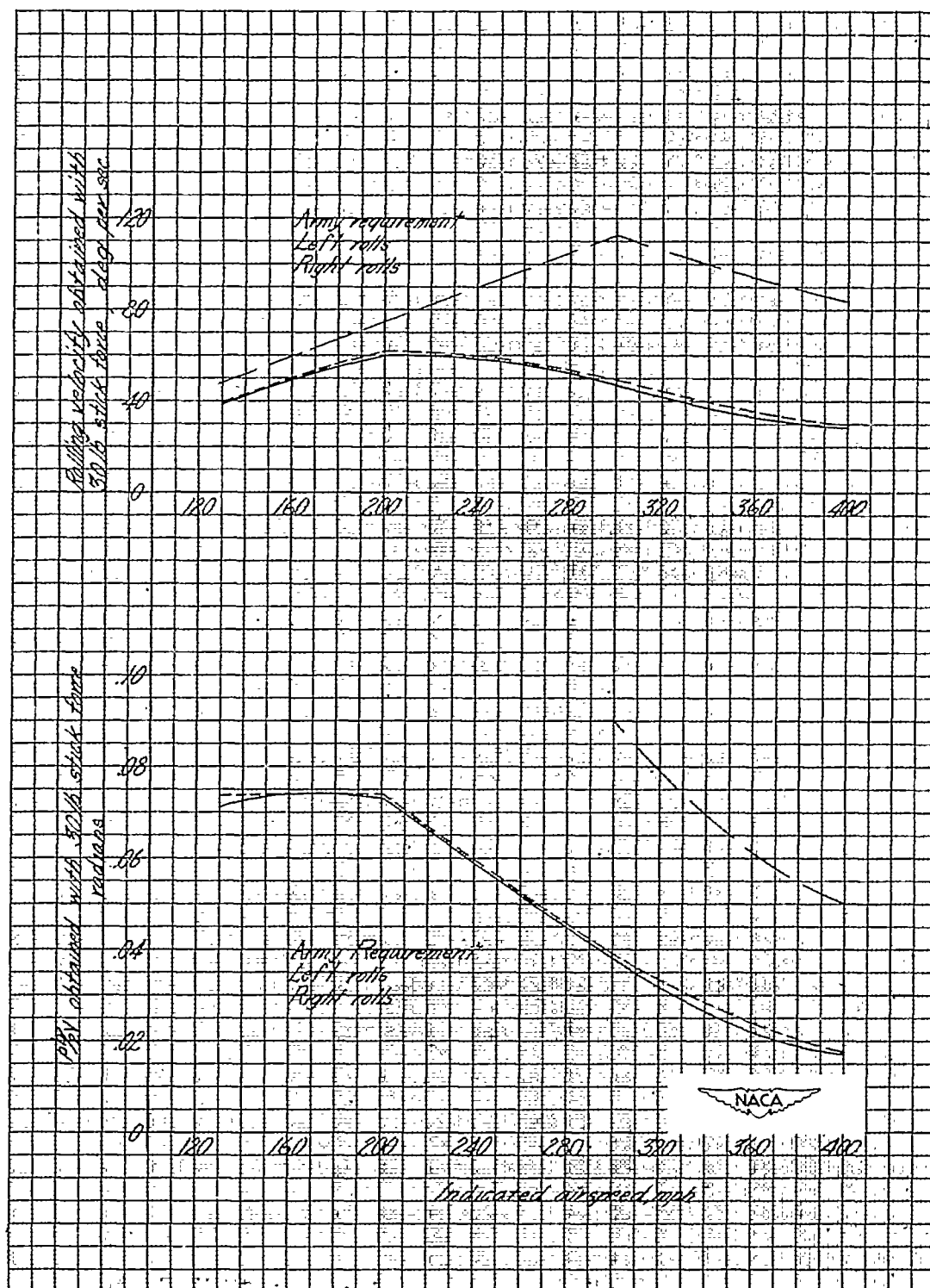
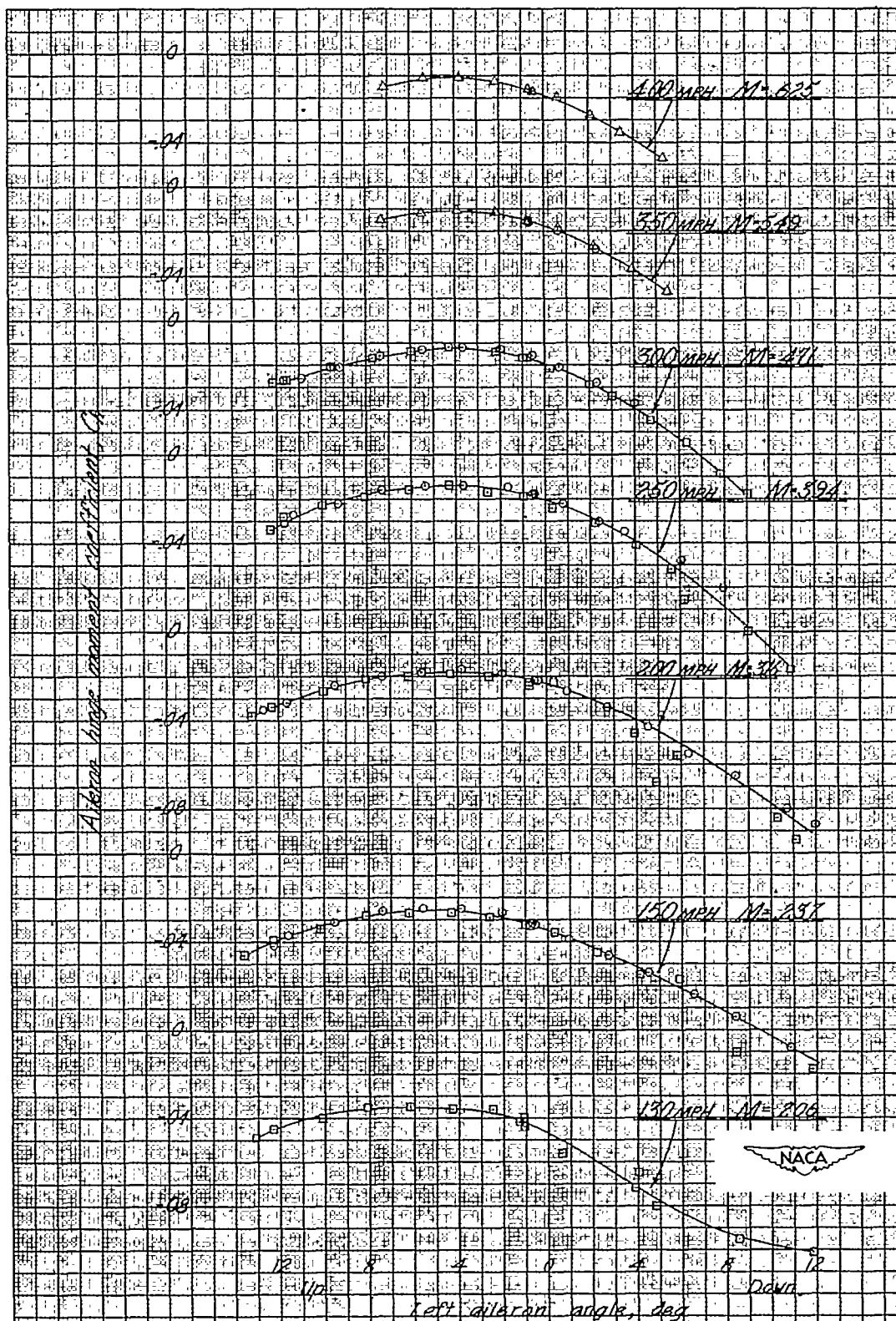


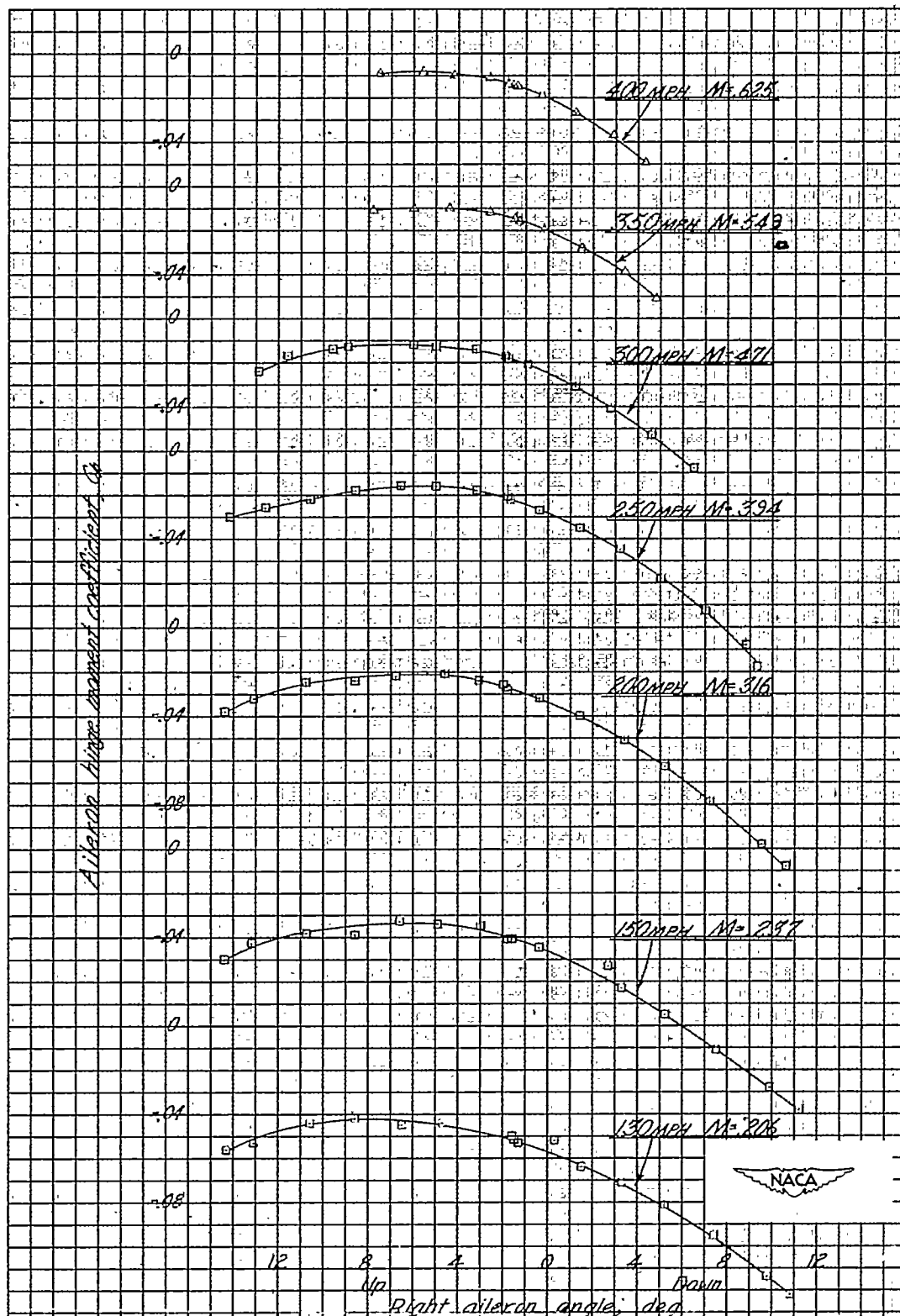
Figure 31.- Variation with indicated airspeed of the helix angle $pb/2V$ and rolling velocity obtained with a 30-pound stick force. F-47D-30 airplane.

8Z



(a) Left aileron. (Different symbols indicate different flights.)

Figure 32.- Variation of aileron hinge-moment coefficient with aileron angle.



(b) Right aileron. (Different symbols indicate different flights.)

Figure 32.- Concluded.

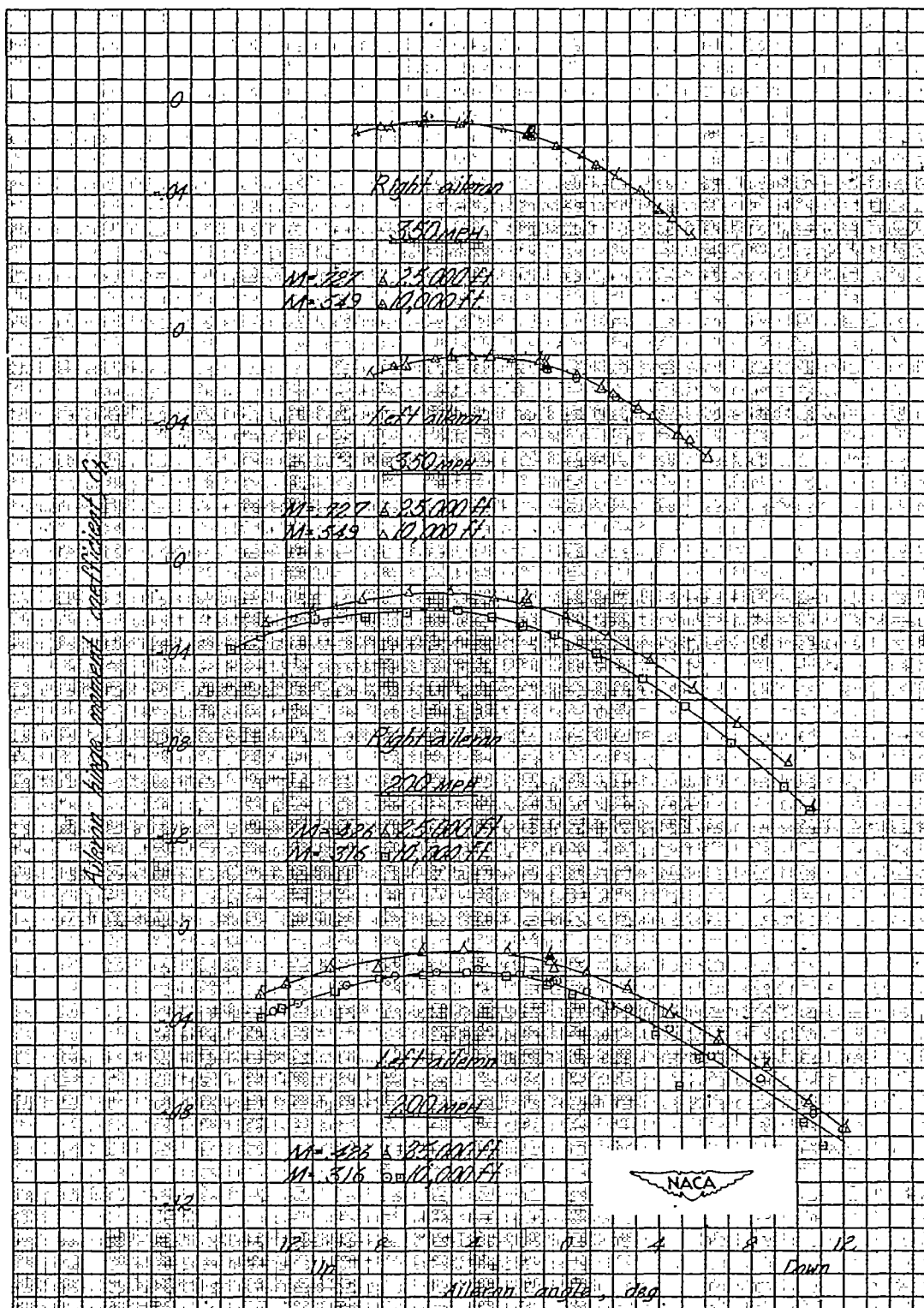


Figure 33.- Effect of altitude on the variation of aileron hinge-moment coefficient with aileron angle. F-47D-30 airplane. (Different symbols indicate different flights.)

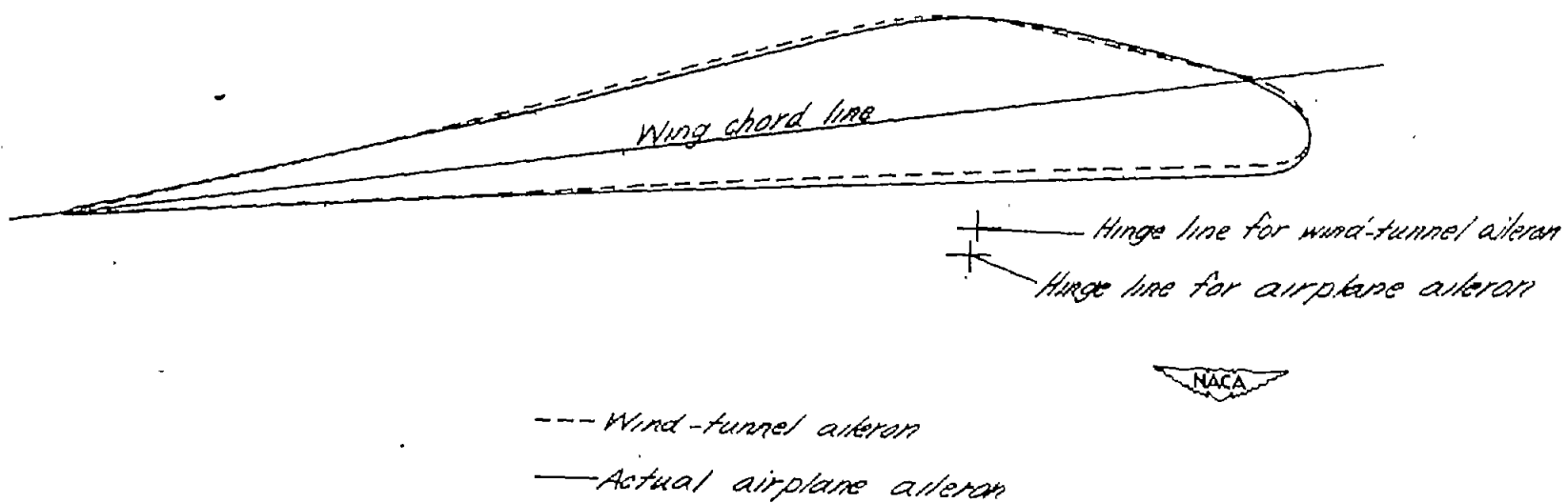


Figure 34.- Profile drawing of the ailerons tested in the wind tunnel and in flight. F-47D-30 ailerons.

9Z

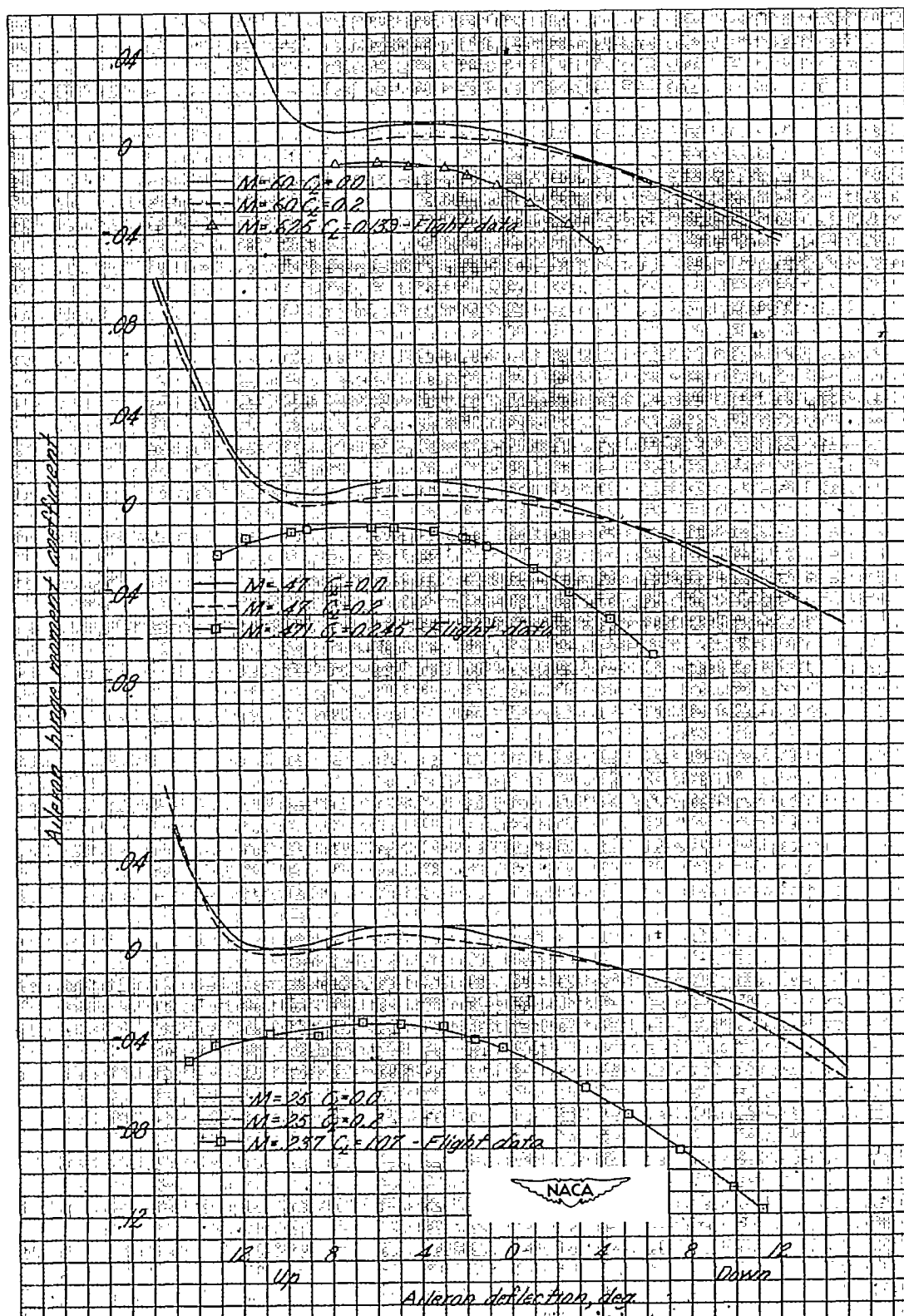


Figure 35.- Comparison of wind-tunnel and flight test data of the aileron hinge-moment characteristics. F-47D-30 airplane; the flight data shown are for the right aileron. The data not labeled flight data are wind-tunnel data.